

# 國立交通大學

## 電信工程學系碩士班 碩士論文

用於時變通道下有限回饋傳送波束形成之  
基於吞吐量模式選擇準則

Throughput-Based Mode Selection Criterion for  
Limited-Feedback Transmit Beamforming over  
Time-Varying Channels

研究生：張亦杰

Student: Yi-Chieh Chang

指導教授：李大嵩 博士

Advisors: Dr. Ta-Sung Lee

吳卓諭 博士

Dr. Jwo-Yuh Wu

中華民國九十八年六月

用於時變通道下有限回饋傳送波束形成之基於吞吐量  
模式選擇準則

Throughput-Based Mode Selection Criterion for  
Limited-Feedback Transmit Beamforming over  
Time-Varying Channels

研 究 生：張亦杰


Student: Yi-Chieh Chang

指 導 教 授：李大嵩 博士

Advisors: Dr. Ta-Sung Lee

吳卓諭 博士

Dr. Jwo-Yuh Wu



國立交通大學

電信工程學系碩士班

碩士論文

A Thesis

Submitted to Department of Communication Engineering

College of Electrical and Computer Engineering

National Chiao Tung University

in Partial Fulfillment of the Requirements

for the Degree of

Master of Science

in

Communication Engineering

June 2009

Hsinchu, Taiwan, Republic of China

中華民國九十八年六月

# 用於時變通道下有限回饋傳送波束形成之基於 吞吐量模式選擇準則

研 究 生：張亦杰

指 導 教 授：李大嵩 博士

吳卓諭 博士

國立交通大學電信工程學系碩士班

## 摘要

在本篇論文中，吾人考慮適用於時變通道環境之多輸入單輸出 (Multiple-Input Single-Output, MISO) 有限回饋預編碼 (Limited Feedback Precoding) 系統的雙模式編碼方法，吾人持用之通道模式係由一階馬可夫通道模型描述。因為通道統計特性隨著時間碼框改變，系統需提供不同大小的碼書以提升性能表現。在吾人的系統中，採用的兩種不同的碼書係遵循 IEEE 802.16e 標準之定義，並分別對應到不同的通道向量量化程度。基於公平原則，系統中的雙模式具有相同的平均回傳率。為了在不同的通道相關性下選擇適當的碼書，吾人提出一個以吞吐量為準則的模式選擇方法協助接收機決定使用的碼書類型。吾人亦提出實際可行的準則實現模式及選擇方法供接收機使用。模擬顯示吾人所提出的模式選擇準則在套用於雙模式系統中可以達到比單模式系統更好的系統性能表現，並可與現有的模式選擇準則相比較。

# Throughput-Based Mode Selection Criterion for Limited-Feedback Transmit Beamforming over Time-Varying Channels

Student: Yi-Chieh Chang

Advisor: Dr. Ta-Sung Lee

Dr. Jwo-Yuh Wu

Department of Communication Engineering

National Chiao Tung University



## Abstract

In this thesis, we consider a dual-mode precoding method for limited-feedback multiple-input single-output (MISO) systems over time-varying channels, which follows the first-order Markov channel model. Since the channel statistics varies over time frames, codebooks of different sizes should be available to improve the system performance. In the considered system, there are two codebooks corresponding to different quantizations of channel vectors as adopted in the IEEE 802.16e standard. For fairness, the two modes have the same feedback rates. To choose one suitable mode for use under different channel correlations, we propose a throughput-based mode selection criterion to help the receiver decide the codebook to be used. A practical way to implement the criterion at the receiver is also proposed. Simulations indicate that the proposed scheme is superior to that with a single codebook and perform comparably to those existing mode selection criteria.

# Acknowledgement

I would like to express my deepest gratitude to my advisors, Dr. Ta-Sung Lee and Dr. Jwo-Yuh Wu, for their training of oral presentation and prudent attitude toward research. Moreover, I learned a lot from their positive attitude in many areas. Thanks are also offered to all members in the Communication System Design and Signal Processing (CSDSP) Lab.

At last but not least, I would like to show my sincere thanks to my family for their invaluable love and support.



# Contents

<b>Contents</b> .....	<b>IV</b>
<b>List of Figures</b> .....	<b>VI</b>
<b>List of Tables</b> .....	<b>VIII</b>
<b>Acronym Glossary</b> .....	<b>IX</b>
<b>Notations</b> .....	<b>X</b>
<b>Chapter 1 Introduction</b> .....	<b>1</b>
<b>Chapter 2 System Model</b> .....	<b>4</b>
2.1 Limited Feedback in MISO System.....	5
2.2 Time-Varying Channel Model .....	6
2.3 Codebook Construction .....	8
2.4 Summary .....	14
<b>Chapter 3 Dual-Mode Scheme and Mode Selection</b> .....	<b>15</b>
3.1 Dual-Mode Scheme .....	16
3.2 Throughput-Based Criterion .....	17
3.3 Modal Metric .....	18
3.3.1 Computation of Modal Metric in Mode I .....	19
3.3.2 Computation of Modal Metric in Mode II.....	21
3.4 Selection of Good Mode and Beamformer .....	25
3.5 Numerical Results.....	26

3.6	Summary .....	28
<b>Chapter 4 Modal Metric Approximation.....</b>		<b>29</b>
4.1	Approximation of Modal Metric in Mode I.....	30
4.2	Approximation of Modal Metric in Mode II.....	34
4.3	Numerical Results .....	37
4.3.1	Approximation vs. Exact Value (Mode I) .....	38
4.3.2	Approximation vs. Exact Value (Mode II).....	39
4.3.3	Dual-Mode Scheme vs. Single-Mode Scheme .....	41
4.3.4	Throughput-Based Criterion vs. Other Criteria .....	43
4.4	Summary .....	45
<b>Chapter 5 Conclusion .....</b>		<b>46</b>
<b>Bibliography .....</b>		<b>48</b>



# List of Figures

Fig. 2-1 MISO system model.....	6
Fig. 2-2 Power spectrum of first order AR process with $a = 0.22$ .....	7
Fig. 3-1 Dual-mode selection scheme in MISO system .....	16
Fig. 3-2 Histogram of the random variable $V$ and its approximation with Gamma distribution .....	23
Fig. 3-3 The RMSE of using $f(v)$ and using different order of polynomials .....	23
Fig. 3-4 Joint PDF of random variables $V$ and $U$ .....	24
Fig. 3-5 Product of PDFs of random variables $V$ and $U$ .....	24
Fig. 3-6 Flow chart of selecting a mode and a beamformer .....	25
Fig. 3-7 Dual-mode scheme and single-mode scheme with SNR = 10dB and 16 QAM .....	27
Fig. 4-1 $T_1$ vs. $T_1^*$ with 16 QAM and different channel correlations .....	38
Fig. 4-2 $T_1$ vs. $T_1^*$ with 64 QAM and different channel correlations .....	39
Fig. 4-3 $T_2$ vs. $T_2^*$ with 16 QAM and different channel correlations .....	40
Fig. 4-4 $T_2$ vs. $T_2^*$ with 64 QAM and different channel correlations .....	40
Fig. 4-5 Dual-mode scheme, Dual-mode scheme with approximated modal metric and single-mode scheme with SNR = 10dB and 16 QAM.....	42
Fig. 4-6 Dual-mode scheme, Dual-mode scheme with approximated modal metric and single-mode scheme with SNR = 10dB and 64 QAM.....	42
Fig. 4-7 Throughput-based criterion and random selection.....	43



Fig. 4-8 Throughput-based criterion and SER-based criterion in the dual-mode scheme with SNR = 10dB and 16 QAM.....44

Fig. 4-9 Throughput-based criterion and SER-based criterion in the dual-mode scheme with SNR = 10dB and 16 QAM.....44



# List of Tables

Table 2-1 Transmit beamforming codebooks in IEEE 802.16-2005 standard.....	8
Table 2-2 MIMO precoding codebook $V(2,1,3)$ .....	8
Table 2-3 MIMO precoding codebook $V(3,1,3)$ .....	9
Table 2-4 MIMO precoding codebook $V(4,1,3)$ .....	9
Table 2-5 Generating parameters for $V(3,1,6)$ and $V(4,1,6)$ .....	10
Table 2-6 MIMO precoding codebook $V(3,1,6)$ .....	11
Table 3-1 Simulation parameters .....	26
Table 4-1 Simulation parameters .....	37



# Acronym Glossary

BER	bit error rate
CSI	channel state information
IEEE	institute of electrical and electronics engineers
MIMO	multiple-input multiple-output
MISO	multiple-input single-output
PDF	probability density function
QAM	quadrature amplitude modulation
SER	symbol error rate
SNR	signal-to-noise ratio



# Notations

$E_s$	average symbol energy
$\mathbb{E}[\cdot]$	expectation operator
$\mathbf{f}_k$	unit precoder for the $k$ th frame
$\mathbf{f}^s$	selected precoder for maximizing the throughput
$\mathcal{F}_1$	3-bit codebook
$\mathcal{F}_2$	6-bit codebook
$\mathbf{h}_k^H$	MISO channel vector for the $k$ th frame
$I_0(\cdot)$	modified Bessel function of the first kind of zero order
$M_{a,b}(\cdot)$	Wittaker function
$n_k$	complex Gaussian noise for the $k$ th frame
$N_t$	number of transmit antennas
$P_M(\gamma)$	symbol error rate for $M$ -QAM modulation
$s_k$	transmitted symbol at the $k$ th frame
$T(\gamma)$	throughput
$T_{i,j}(\gamma)$	throughput for the $i$ th frame under the $j$ th mode
$y_k$	received signal at the the $k$ th frame
$\gamma$	instantaneous signal-to-noise ratio
$\Gamma(\cdot)$	gamma function
$\Gamma_m$	modal metric for the $m$ th mode
$\Delta\mathbf{h}$	innation vector for the first-order Markov channel model
$\rho$	channel correlation
$\Phi(\cdot)$	confluent hypergeometric function

# Chapter 1

## Introduction

In wireless transmission scenarios, multiple antennas at both the transmitter and the receiver are employed to provide higher data transmission rate and lower data error rate, and this is known as multiple-input multiple-output (MIMO) systems. There are two types of scenario in MIMO systems, which are open-loop systems and closed-loop systems. For the former one, the receiver does not use channel state information (CSI), while the latter is able to acquire CSI from the receiver. Among open-loop architectures, one of the most popular approaches is the Vertical Bell Laboratories Layered Space-Time (V-BLAST) [1], which involves a simple coding technique to send data via different data streams, and hence enhance the data transmission rate. Closed-loop systems, while having CSI at the transmitter and hence increasing the complexity of the receiver, yield higher capacities and lower data error rate since the transmitted data can be pre-designed to match the channel. Limited feedback scenario thus arises as a topic for closed-loop systems and the goal is to provide a way to feed back the CSI from the receiver to the transmitter much efficiently and reliably [2, 3]. Another important issue in limited feedback systems is the codebook design, which discusses the problem of quantizing the perfect channel vector so that the receiver can feed back CSI over a bandlimited channel.

In multiple antenna systems, beamforming is a simple technique to improve system performance in fading channels [4, 5]. Unfortunately, this scheme needs perfect CSI, which is often not available at the transmitter side, to achieve the theoretical performance. Previous works [6-8] have investigated many ways to feed back the CSI to transmitter. For example, the mean-feedback technique is discussed in [6, 7]; the covariance-feedback approach is presented in [6, 8]. Among these works, they assume the transmitter has the knowledge of channel distribution, so the first-order and second-order statistics are fed back to improve the system performance. In this thesis, we focus on one prevailing technique in which the quantized channel vectors lying in pre-designed codebooks are fed back to the transmitter [4, 9], and this kind of scheme were adopted in systems like the IEEE 802.16e standard [10].

We consider a precoding scheme called dual-mode precoding method in [11] with a different mode selection criterion, based on throughput consideration. Under the architecture of dual-mode precoding, two codebooks containing different number of quantized channel vectors are provided at both the transmitter and the receiver. The receiver chooses not only the best precoder in terms of throughput, which will be defined in Chapter 3, but also a suitable mode for the transmitter to adopt. Here, different modes correspond to different codebooks, which in our case are 3-bit quantization codebook and 6-bit quantization codebook as adopted in the IEEE 802.16e standard [10]. As for mode selection, the modal metric exploiting channel correlation will be defined in this thesis, which is similar to that in [11]. Simulations indicate that the proposed criterion works well for the dual-mode scheme and is superior to the system having only one codebook, which we call the single-mode scheme throughout this thesis. Also, the dual-mode scheme with the proposed criterion has comparable performance to other existing criteria and is of more practical interests.

This thesis will proceed as follows. Chapter 2 describes the system model and the channel model used in our work. Also, the codebook construction in IEEE 802.16e-2005 is presented. In Chapter 3, we will give the definition of the throughput and the modal metric. Moreover, the throughput-based mode selection criterion will be defined and the computation of the modal metric with respect to Mode I and Mode II are also presented. In Chapter 4, the accurate approximations of the modal metric pertaining to the two modes will be derived, which is proved to be accurate in terms of numerical experiment. Simulations and conclusions are presented in Chapter 4 and Chapter 5, respectively.



# Chapter 2

## System Model

Limited feedback system was first proposed in [2, 3] and has drawn attention for many years and emerged as one of the most significant techniques in wireless communications. A great many research works have investigated its utility and justified the great performance enhancement via limited bits fed back to the transmitter. Moreover, limited feedback scheme has been employed in multiple-input multiple-output (MIMO) systems to provide higher capacity and higher reliability in recent years since channel state information (CSI) can be relayed back to the transmitter in an efficient way.

One of the greatest challenges of designing limited-feedback scheme lies in the design of codebooks. How to design codebooks so that the matrices in them can best describe the channel quality in various circumstances has been discussed and solved. In [12], the codebook design criterion in independent and identically distributed Rayleigh fading matrix channels is related to the problem of Grassmannian line packing. Also, the random vector quantization (RVQ) technique is introduced in [13] to provide a simple approach to codebook design. Moreover, a systematic codebook design for correlated channels is presented in [14].



In Chapter 2, a limited feedback scheme in MISO system is introduced first. Then, a time-varying channel model, which in our case is the first-order Markov channel model, will be given and discussed. Finally, IEEE 802.16-2005 [10] codebook construction is presented

## 2.1 Limited Feedback in MISO System

We consider a multi-input single-output (MISO) system with  $N_t$  transmit antennas and a single receive antenna, which is shown in Fig. 2-1. The received signal can be described as

$$y_k = \mathbf{h}_k^H \mathbf{f}_k s_k + n_k \quad (2.1)$$

where  $s_k$  is the transmitted symbol at  $k$ th frame and  $\mathbf{f}_k$  is an  $N_t \times 1$  unit precoder which is selected for the same frame. Channel vector is described as  $\mathbf{h}_k^H = [h_1^H, h_2^H, \dots, h_{N_t}^H]$  and  $\mathbf{h}_k^H \sim \mathcal{CN}(\mathbf{0}_{N_t}, \mathbf{I}_{N_t})$  is distributed according to complex Gaussian distribution with zero mean and unit variance. Also, we assume the received signal experiences the noise  $n_k \sim \mathcal{CN}(0, N_0)$  at the receiver.

Assuming that the receiver has full knowledge of channel statistics, the instantaneous signal-to-noise ratio (SNR) in (2.1) is

$$\gamma = \left| \mathbf{h}_k^H \mathbf{f}_k \right|^2 \frac{Es}{N_0} \quad (2.2)$$

with  $Es$  denoting the average symbol energy. In the following, we will assume that  $Es = 1$ .

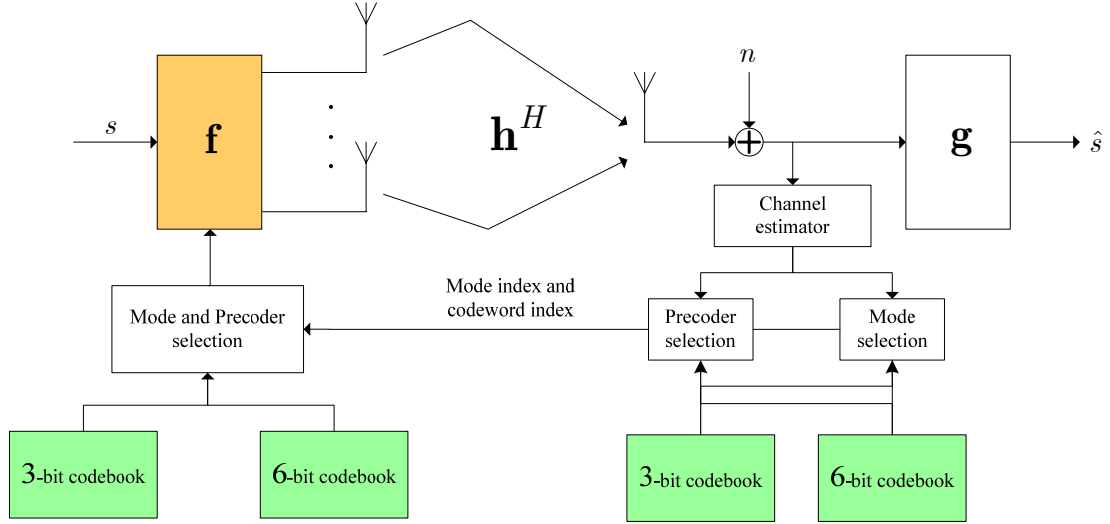


Fig. 2-1 MISO system model

## 2.2 Time-Varying Channel Model

The channel model used in this thesis follows the first-order Markov channel model [15-17]

$$\mathbf{h}_{k+1} = \sqrt{\rho}\mathbf{h}_k + \Delta\mathbf{h} \quad (2.3)$$

where  $\Delta\mathbf{h} \sim \mathcal{CN}(\mathbf{0}_{N_t}, (1-\rho)\mathbf{I}_{N_t})$  is the innovation vector and  $\rho$  is the channel correlation between  $k$ th and  $(k+1)$ th frame, in which  $k$  denotes a specific frame index.

In fact, (2.3) can be viewed as a first-order autoregressive (AR) process [15], which is often used to approximate a given random process. A complex AR process can be generated via the following recursion formula

$$x[n] = \sum_{k=1}^p a_k x[n-k] + w[n] \quad (2.4)$$

where  $p$  is the order of AR and  $w[n]$  is the innovation vector, which is complex white Gaussian with zero mean and variance  $\sigma^2$ . Comparing (2.3) with (2.4), we immediately verify that our channel model is equivalent to a first-order AR process.

The corresponding power spectrum density (PSD) of the AR process has the

following rational form [17]:

$$S_{xx}(f) = \frac{\sigma^2}{\left|1 - \sum_{k=1}^p a_k \exp(-j2\pi fk)\right|^2} \quad -\frac{1}{2} \leq f \leq \frac{1}{2} \quad (2.5)$$

which is bell-shaped (see Fig. 2-2) and can be used to approximate indoor channel models [18]

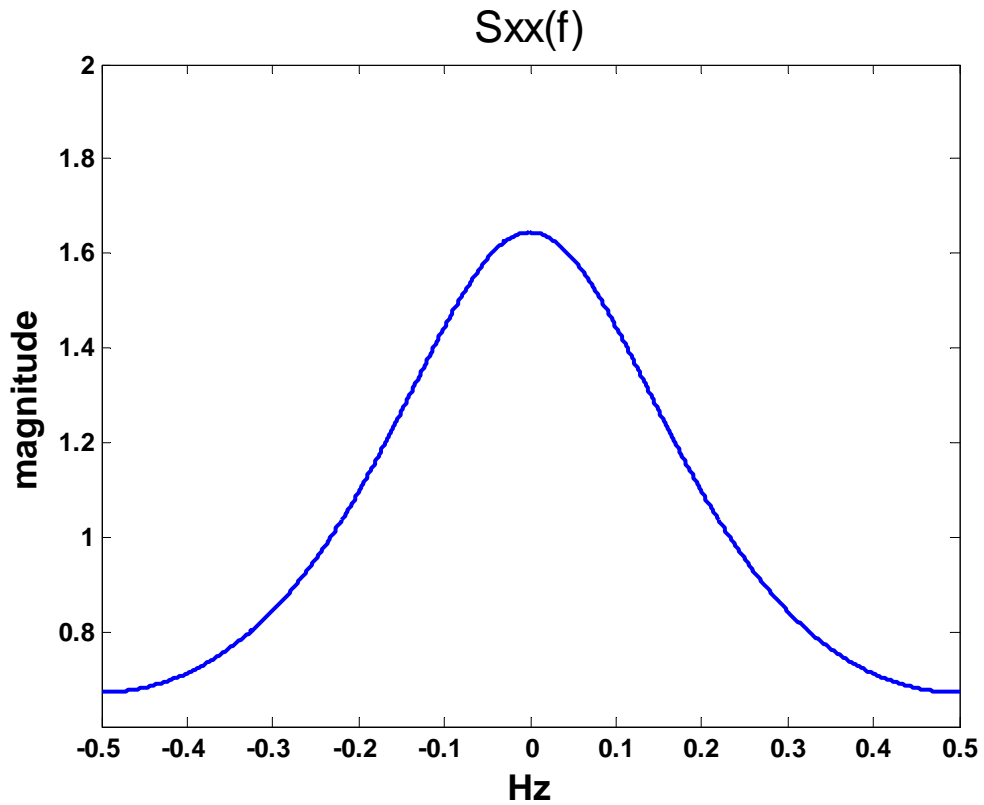


Fig. 2-2 Power spectrum of first order AR process with a = 0.22

## 2.3 Codebook Construction

There are two kinds of codebooks defined in the the IEEE 802.16-2005 standard [10]: 3-bit codebooks and 6-bit codebooks. When both the number of input data streams and the number of the receive antennas are equal to 1, the scenario is called transmit beamforming. The transmit beamforming codebooks are listed in Table 2-1. The notation  $V(N_t, S, L)$  denotes the vector codebook, which consists of  $2^L$  complex unit vectors of dimension  $N_t$ . The  $S$  denotes the number of substreams. All the codewords of  $V(2,1,3)$ ,  $V(3,1,3)$ , and  $V(4,1,3)$  are listed in Table 2-2, Table 2-3, and Table 2-4.

Table 2-1 Transmit beamforming codebooks in the IEEE 802.16-2005 standard

$N_t, S \setminus L$	<b>3</b>	<b>6</b>
<b>2,1</b>	$V(2,1,3)$	$V(2,1,6)$
<b>3,1</b>	$V(3,1,3)$	$V(3,1,6)$
<b>4,1</b>	$V(4,1,3)$	$V(4,1,6)$

Table 2-2 MIMO precoding codebook  $V(2,1,3)$

Vector index	1	2	3	4	5	6	7	8
v1	1	0.7490	0.7490	0.7491	0.7491	0.3289	0.05112	0.3289
v2	0	-0.5801 +j0.1818	0.0576 +j0.6051	-0.2978 -j0.5298	-0.6038 +j0.0689	-0.6614 +j0.6740	-0.4754 -j0.7160	-0.8779 -j0.3481

Table 2-3 MIMO precoding codebook  $V(3,1,3)$ 

Vector index	1	2	3	4	5	6	7	8
v1	1	0.5	0.5	0.5	0.5	0.4954	0.5	0.5
v2	0	-0.7201 -0.3126i	-0.0659 +0.1371i	-0.0063 +0.6527i	0.7171 +0.3202i	0.4819 -0.4517i	0.0686 -0.1386i	-0.0054 -0.654i
v3	0	0.2483 -0.2684i	-0.6283 -0.5763i	0.4621 -0.3321i	-0.2533 +0.2626i	0.2963 -0.4801i	0.6200 +0.5845i	-0.4566 +0.3374i

Table 2-4 MIMO precoding codebook  $V(4,1,3)$ 

Vector index	1	2	3	4	5	6	7	8
v1	1	0.3780	0.3780	0.3780	0.3780	0.3780	0.3780	0.3780
v2	0	-0.2698 -0.5668i	-0.7103 +0.1326i	0.2830 -0.094i	-0.0841 +0.6478i	0.5247 +0.3532i	0.2058 -0.1369i	0.0618 -0.3332i
v3	0	0.5957 +0.1578i	-0.235 -0.1467i	0.0702 -0.8261i	0.0184 +0.049i	0.4115 +0.1825i	-0.5211 +0.0833i	-0.3456 +0.5029i
v4	0	0.1587 -0.2411i	0.1371 +0.4893i	-0.2801 +0.0491i	-0.3272 -0.5662i	0.2639 +0.4299i	0.6136 -0.3755i	-0.5704 +0.2133i

In the IEEE 802.16-2005 standard [10], two vector codebooks  $V(3,1,6)$  and  $V(4,1,6)$  are generated as follows. All the vector codewords  $\mathbf{v}_i$ ,  $i = 2, \dots, 2^L$  are derived from the first codeword  $\mathbf{v}_1$  as

$$\tilde{\mathbf{v}}_i = H(\mathbf{s})Q^i(\mathbf{u})H^H(\mathbf{s})\mathbf{v}_{i-1}, \text{ for } i = 2, \dots, 2^L, \quad (2.6)$$

$$\mathbf{v}_i = \tilde{\mathbf{v}}_i e^{-j\phi_i}, \text{ for } i = 2, \dots, 2^L, \quad (2.7)$$

where  $Q^i(\mathbf{u}) = \text{diag} \left( e^{j \frac{2\pi}{2^L} u_1 \cdot i}, \dots, e^{j \frac{2\pi}{2^L} u_{N_t} \cdot i} \right)$  is a diagonal matrix,  $\mathbf{u} = [u_1, \dots, u_{N_t}]$

is an integer vector,  $\mathbf{v}_1 = \frac{1}{\sqrt{N_t}} \left[ 1, e^{j \frac{2\pi}{N_t}}, \dots, e^{j \frac{2\pi}{N_t} (N_t-1)} \right]^T$ , and  $\phi_i$  is the phase of the

first entry of  $\tilde{\mathbf{v}}_i$ .  $H(\cdot)$  is defined as

$$H(\mathbf{v}) = \begin{cases} \mathbf{I}, & \mathbf{v} = \mathbf{e}_1 \\ I - p\mathbf{w}\mathbf{w}^H, & \text{otherwise} \end{cases}, \quad (2.8)$$

where  $\mathbf{w} = \mathbf{v} - \mathbf{e}_1$ ,  $\mathbf{e}_1 = [1, 0, \dots, 0]^T$ ,  $p = \frac{2}{\|\mathbf{w}^H \mathbf{w}\|^2}$ , and  $\mathbf{I}$  is the identity matrix.

The parameters for the generation of  $V(3,1,6)$  and  $V(4,1,6)$  are listed in Table 2-5 and the codewords of  $V(3,1,6)$  is listed in Table 2-6.

Table 2-5 Generating parameters for  $V(3,1,6)$  and  $V(4,1,6)$

$N_t$	$L$	$\mathbf{u}$ in $Q^i(\mathbf{u})$	$\mathbf{s}$ in $H(\mathbf{s})$
3	6	[1, 26, 57]	$[1.2518 - j0.6409, -0.4570 - j0.4974, 0.1177 + j0.2360]^T$
4	6	[1, 45, 22, 49]	$[1.3954 - j0.0738, 0.0206 + j0.4326,$ $-0.1658 - j0.5445, 0.5487 - j0.1599]^T$

The algorithms given above can help us generate the vector codebooks  $V(3,1,6)$  and  $V(4,1,6)$ . But, the IEEE 802.16e-2005 standard does not provide the generating parameters for the codebook  $V(2,1,6)$ .

There are sixty-four precoders in the 6-bit codebook to be selected. Therefore it has a higher probability that a near-optimal precoder can be selected. But the receiver needs to feed back six bits per CSI update. On the other hand, although the 3-bit codebook provides only eight beamformers to be selected, the feedback amount per CSI update is only three bits.

Table 2-6 MIMO precoding codebook  $V(3,1,6)$

Matrix index (binary)	Column 1	Matrix index(binary)	Column 1
000000	0.5774	100000	0.5437
	$-0.2887 + j0.5000$		$-0.1363 - j0.4648$
	$-0.2887 - j0.5000$		$0.4162 + j0.5446$
000001	0.5466	100001	0.5579
	$0.2895 - j0.5522$		$-0.6391 + j0.3224$
	$0.2440 + j0.5030$		$-0.2285 - j0.3523$
000010	0.5246	100010	0.5649
	$-0.7973 - j0.0214$		$0.6592 - j0.3268$
	$-0.2517 - j0.1590$		$0.1231 + j0.3526$
000011	0.5973	100011	0.484
	$0.7734 + j0.0785$		$-0.6914 - j0.3911$
	$0.1208 + j0.1559$		$-0.3669 + j0.0096$
000100	0.4462	100100	0.6348
	$-0.3483 - j0.6123$		$0.5910 + j0.4415$
	$-0.5457 + j0.0829$		$0.2296 - j0.0034$
000101	0.6662	100101	0.4209
	$0.2182 + j0.5942$		$0.0760 - j0.5484$
	$0.3876 - j0.0721$		$-0.7180 + j0.0283$
000110	0.412	100110	0.6833
	$0.3538 - j0.2134$		$-0.1769 + j0.4784$
	$-0.8046 - j0.1101$		$0.5208 - j0.0412$
000111	0.684	100111	0.4149
	$-0.4292 + j0.1401$		$0.3501 + j0.2162$
	$0.5698 + j0.0605$		$-0.7772 - j0.2335$
001000	0.4201	101000	0.6726
	$0.1033 + j0.5446$		$-0.4225 - j0.2866$
	$-0.6685 - j0.2632$		$0.5061 + j0.1754$
001001	0.6591	101001	0.419
	$-0.1405 - j0.6096$		$-0.2524 + j0.6679$
	$0.3470 + j0.2319$		$-0.5320 - j0.1779$
001010	0.407	101010	0.6547
	$-0.5776 + j0.5744$		$0.2890 - j0.6562$
	$-0.4133 + j0.0006$		$0.1615 + j0.1765$

Table 2-6 MIMO precoding codebook  $V(3,1,6)$  (continued)

Matrix index (binary)	Column 1	Matrix index(binary)	Column 1
001011	0.6659	101011	0.3843
	$0.6320 - j0.3939$		$-0.7637 + j0.3120$
	$0.0417 + j0.0157$		$-0.3465 + j0.2272$
001100	0.355	101100	0.69
	$-0.7412 - j0.029$		$0.6998 + j0.0252$
	$-0.3542 + j0.445$		$0.0406 - j0.1786$
001101	0.7173	101101	0.3263
	$0.4710 + j0.3756$		$-0.4920 - j0.3199$
	$0.1394 - j0.3211$		$-0.4413 + j0.5954$
001110	0.307	101110	0.7365
	$-0.0852 - j0.414$		$0.0693 + j0.4971$
	$-0.5749 + j0.629$		$0.2728 - j0.3623$
001111	0.74	101111	0.3038
	$-0.3257 + j0.346$		$0.3052 - j0.2326$
	$0.3689 - j0.3007$		$-0.6770 + j0.5496$
010000	0.3169	110000	0.727
	$0.4970 + j0.1434$		$-0.5479 - j0.0130$
	$-0.6723 + j0.424$		$0.3750 - j0.1748$
010001	0.7031	110001	0.3401
	$-0.4939 - j0.429$		$0.4380 + j0.5298$
	$0.2729 - j0.0509$		$-0.5470 + j0.3356$
010010	0.3649	110010	0.6791
	$0.1983 + j0.7795$		$-0.1741 - j0.7073$
	$-0.3404 + j0.3224$		$0.0909 - j0.0028$
010011	0.6658	110011	0.3844
	$0.2561 - j0.6902$		$-0.1123 + j0.8251$
	$-0.0958 - j0.0746$		$-0.1082 + j0.3836$
010100	0.3942	110100	0.6683
	$-0.3862 + j0.6614$		$0.5567 - j0.3796$
	$0.0940 + j0.4992$		$-0.2017 - j0.2423$
010101	0.6825	110101	0.394
	$0.5632 + j0.0490$		$-0.5255 + j0.3339$
	$-0.1901 - j0.4225$		$0.2176 + j0.6401$



Table 2-6 MIMO precoding codebook  $V(3,1,6)$  (continued)

Matrix index (binary)	Column 1	Matrix index(binary)	Column 1
010110	0.3873	110110	0.6976
	$-0.4531 - j0.0567$		$0.2872 + j0.3740$
	$0.2298 + j0.7672$		$-0.0927 - j0.5314$
010111	0.7029	110111	0.3819
	$-0.1291 + j0.4563$		$-0.1507 - j0.3542$
	$0.0228 - j0.5296$		$0.1342 + j0.8294$
011000	0.387	111000	0.6922
	$0.2812 - j0.3980$		$-0.5051 + j0.2745$
	$-0.0077 + j0.7828$		$0.0904 - j0.4269$
011001	0.6658	111001	0.4083
	$-0.6858 - j0.0919$		$0.6327 - j0.1488$
	$0.0666 - j0.2711$		$-0.0942 + j0.6341$
011010	0.4436	111010	0.6306
	$0.7305 + j0.2507$		$-0.5866 - j0.4869$
	$-0.0580 + j0.4511$		$-0.0583 - j0.1337$
011011	0.5972	111011	0.4841
	$-0.2385 - j0.7188$		$0.5572 + j0.5926$
	$-0.2493 - j0.0873$		$0.0898 + j0.3096$
011100	0.5198	111100	0.5761
	$0.2157 + j0.7332$		$0.1868 - j0.6492$
	$0.2877 + j0.2509$		$-0.4292 - j0.1659$
011101	0.571	111101	0.5431
	$0.4513 - j0.3043$		$-0.1479 + j0.6238$
	$-0.5190 - j0.3292$		$0.4646 + j0.2796$
011110	0.5517	111110	0.5764
	$-0.3892 + j0.3011$		$0.4156 + j0.1263$
	$0.5611 + j0.3724$		$-0.4947 - j0.4840$
011111	0.5818	111111	0.549
	$0.1190 + j0.4328$		$-0.3963 - j0.1208$
	$-0.3964 - j0.5504$		$0.5426 + j0.4822$

## 2.4 Summary

In this chapter, the limited-feedback MISO system in our work is introduced. In particular, two codebooks of different sizes are considered in the system. Then, we introduce and analyze the first-order Markov channel model. Moreover, codebook construction in the IEEE 802.16e-2005 standard is also presented. Finally, since there are two kinds of sizes of codebooks in the standard, this gives us the motivation how to design a scheme to utilize them in time varying channels, and the proposed algorithm will be presented in Chapter 3.



# Chapter 3

## Dual-Mode Scheme and Mode Selection

In our work, we have two codebooks  $\mathcal{F}_1$  and  $\mathcal{F}_2$  corresponding to 6-bit quantization and 3-bit quantization at the receiver and the transmitter. For simplicity, we call the mode using the 6-bit codebook for limited feedback as Mode I and the mode using the 3-bit codebook as Mode II. The two modes are defined as follows: (1) Under Mode I scheme, the best precoder is chosen at the receiver, and then the index of the precoder, which is coded in 6 bits, are fed back to the transmitter per two frames; (2) For Mode II, this work is realized per one frame. Therefore, the two modes in our definition have the same feedback rate as 3 bits/time frame.

Instead of using Mode I or Mode II exclusively for the system architecture, we consider a dual-mode scheme in [11], in which two codebooks are available at both the transmitter and the receiver, to improve the defects in the single-mode scheme that neither Mode I nor Mode II performs well at all channel correlations. Moreover, we propose a selection criterion base on throughput to adaptively switch between Mode I and Mode II and take the advantages of each mode in various channel correlations. Finally, simulations are given to verify the proposed method.

### 3.1 Dual-Mode Scheme

The dual-mode limited feedback system has two codebooks of different sizes at the receiver and transmitter. In this thesis, we adopt the 3-bit and 6-bit codebooks in the IEEE 802.16e-2005 [10], which have been introduced in Chapter 2. In order to fairly compare between the two modes and select one for use, we consider a fixed-rate feedback scheme as described in [11]. Namely, 6 bits are fed back to the transmitter per two frames in Mode I; 3 bits are fed back to the transmitter per one frame in Mode II. As a result, an equal feedback rate of 3 bits/frame is maintained for each mode. In particular, we assume that the transmitter is able to distinguish between the two modes via feedback bits without extra ones for indicating which mode should be adopted. Also, we assume that the receiver has full knowledge of CSI at the start of each frame so that it can choose the best beamformer and better mode for use in time-varying channel. The dual-mode selection scheme in MISO system is shown in Fig. 3-1

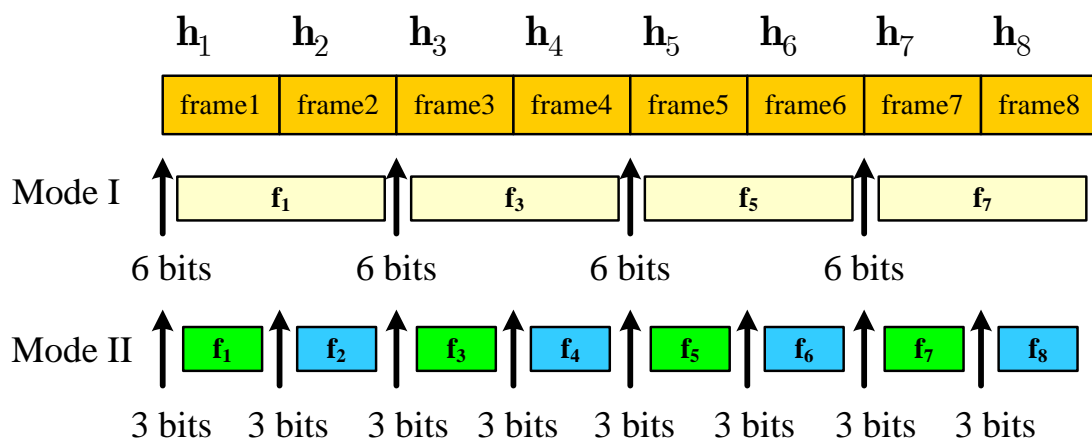


Fig. 3-1 Dual-mode selection scheme in MISO system

## 3.2 Throughput-Based Criterion

Before a further discussion, we should first define the throughput used in this work. The throughput is defined as (maximum reliable transmission rate)  $\times$  (1 - bit error rate), whose physical meaning is the number of correct bits per second that can be achieved without any error-control coding if the transmitter use the channel capacity as the transmission rate. The maximum reliable transmission rate is channel capacity

$$C(\gamma) = \log_2(1 + \gamma) \quad (3.1)$$

where  $\gamma$  is given by (2.2).

The bit error rate (BER) generally has no closed-form solution, therefore we turn to its upper bound from the relation with symbol error rate (SER)

$$\frac{\text{SER}}{\log_2 M} \leq \text{BER} \leq \text{SER}. \quad (3.2)$$

Considering the worst case, we choose SER as BER.

Finally the throughput is written as

$$T(\gamma) = C(\gamma) \cdot (1 - P_M(\gamma)) \quad (3.3)$$

where  $P_M(\gamma)$  is the SER for a given modulation scheme, which is  $M$ -QAM in our case, and has the following formula [19]:

$$P_M(\gamma) = 1 - \left( 1 - 2 \left( 1 - \frac{1}{\sqrt{M}} \right) Q \left( \sqrt{\frac{3}{M-1}} \gamma \right) \right)^2. \quad (3.4)$$

Therefore, with (3.1) and (3.4), the throughput becomes

$$T(\gamma) = \log_2(1 + \gamma) \cdot \left( 1 - 2 \left( 1 - \frac{1}{\sqrt{M}} \right) Q \left( \sqrt{\frac{3}{M-1}} \gamma \right) \right)^2. \quad (3.5)$$

### 3.3 Modal Metric

In order to select a better mode for use at the transmitter, we should first define the modal metric used at the receiver. Modal metric, as implied by its name, is used as a gauge to compare between two modes, and a careful choice of it can increase the system performance. Our modal metric is defined as the average throughput between two consecutive frames:

$$\Gamma_m = \frac{1}{2} \{T_{k,m}(\gamma) + \mathbb{E}[T_{k+1,m}(\gamma)]\}, \quad m \in \{1,2\} \quad (3.6)$$

where  $T_{i,j}(\gamma)$  is the throughput for the  $i$ th frame under the  $j$ th mode and  $\mathbb{E}[\cdot]$  denotes expectation over channel statistics. This type of modal metric is also defined in [11] in which the modal metric is defined as

$$\Gamma_m = \frac{1}{2} \{SER_{k,m}(\gamma) + \mathbb{E}[SER_{k+1,m}(\gamma)]\}, \quad m \in \{1,2\} \quad (3.7)$$

where  $SER_{i,j}(\gamma)$  is the SER for the  $i$ th frame under the  $j$ th mode. Therefore, the selection criterion in [11] is called SER-based criterion.

The reason for the expectation is based on the fact that we assume the receiver has full knowledge of channel statistics at  $k$ th frame but nothing about it for the coming frame. Taking average over two time frames can help the receiver exploit the information of channel correlation and further enhance the accuracy of our modal metric. If the channel correlation  $\rho$  is equal to 1, then there is no need to take the expectation over the  $(k+1)$ th frame, so the modal metric in this case becomes

$$\Gamma_m = T_{k,m}(\gamma) \quad m \in \{1,2\} \quad (3.8)$$

### 3.3.1 Computation of Modal Metric in Mode I

The expected value of the throughput corresponding to Mode I conditioned on  $\mathbf{h}_k$  can be formulated as

$$\mathbb{E}[T_{k+1,1}(\gamma)] = \int_0^\infty T_{k+1,1}(\gamma) \cdot f_\Gamma(\gamma|\mathbf{h}_k) d\gamma \quad (3.9)$$

where  $\gamma = |\mathbf{h}_{k+1}^H \mathbf{f}_{k+1}^s|^2 / N_0$  and  $f_\Gamma(\gamma|\mathbf{h}_k)$  is the probability density function (PDF) of the random variable  $\Gamma$  conditioned on  $\mathbf{h}_k$ . In order to compute this integral, we need to find out the distribution of  $\Gamma$ .

In this mode, the selected precoder for the  $(k+1)$ th frame is the same to that for the previous one, i.e.,  $\mathbf{f}_{k+1}^s = \mathbf{f}_k^s$ , therefore, we can rewrite  $\gamma$  as  $|\mathbf{h}_{k+1}^H \mathbf{f}_k^s|^2 / N_0$ .

Furthermore, we transform (3.9) into another representation

$$\mathbb{E}[T_{k+1,1}(\gamma)] = \int_0^\infty T\left(\frac{y}{N_0}\right) \cdot f_Y(y|\mathbf{h}_k) dy \quad (3.10)$$

where  $Y = |\mathbf{h}_{k+1}^H \mathbf{f}_k^s|^2$  and  $f_Y(y|\mathbf{h}_k)$  is the PDF of random variable  $Y$  conditioned on  $\mathbf{h}_k$ . The derivation of  $f_Y(y|\mathbf{h}_k)$  can be found in [11] and is illustrated as follows.

Replacing  $\mathbf{h}_{k+1}$  with  $\sqrt{\rho}\mathbf{h}_k + \Delta\mathbf{h}$  in  $\mathbf{h}_{k+1}^H \mathbf{f}_k^s$ , we obtain

$$\mathbf{h}_{k+1}^H \mathbf{f}_k^s = (m_R + jm_I) + (\Delta h_R + j\Delta h_I) \quad (3.11)$$

where  $(m_R + jm_I) = \sqrt{\rho}\mathbf{h}_k^H \mathbf{f}_k^s$  and  $\Delta h_R + j\Delta h_I = \Delta\mathbf{h}_k^H \mathbf{f}_k^s$ . Due to the fact that

$\|\mathbf{f}\|^2 = 1$  and  $\Delta\mathbf{h} \sim \mathcal{CN}(\mathbf{0}_{N_t}, (1-\rho)\mathbf{I}_{N_t})$ , we have  $\Delta h_R \sim \mathcal{N}(0, \frac{1-\rho}{2})$  and

$\Delta h_I \sim \mathcal{N}(0, \frac{1-\rho}{2})$ . If we denote  $(m_R + \Delta h_R)$  and  $(m_I + \Delta h_I)$  as  $X_R$  and

$X_I$  respectively, then  $X_R \sim \mathcal{N}(m_R, \frac{1-\rho}{2})$  and  $X_I \sim \mathcal{N}(m_I, \frac{1-\rho}{2})$  since both

$m_R$  and  $m_I$  are deterministic. Moreover, let

$$Z = \frac{X_R^2}{(1-\rho)/2} + \frac{X_I^2}{(1-\rho)/2} = \frac{2}{1-\rho} Y \quad (3.12)$$

then we find that  $Z$  is a noncentral Chi-square distributed random variable with degrees of freedom being 2 and the noncentrality parameter being  $\lambda$  [20]

$$\lambda = \frac{(m_R)^2}{(1-\rho)/2} + \frac{(m_I)^2}{(1-\rho)/2} = \frac{2}{1-\rho} \left| \sqrt{\rho} \mathbf{h}_k^H \mathbf{f}_k^s \right|^2. \quad (3.13)$$

Therefore, the PDF of  $Y$  can be directly obtained from  $Z$

$$f_Y(y | \mathbf{h}_k) = \frac{dF_Y(y | \mathbf{h}_k)}{dy} = \frac{dF_Z(y/a)}{dy} = \frac{1}{a} f_Z\left(\frac{y}{a}\right) \quad (3.14)$$

where  $a = \frac{1-\rho}{2}$ , and  $f_Z(z)$  is the PDF of random variable  $Z$

$$f_Z(z) = \frac{1}{2} \exp\left(\frac{-(z+\lambda)}{2}\right) \cdot I_0(\sqrt{\lambda z}). \quad (3.15)$$

$I_0(\cdot)$  is the modified Bessel function of the first kind of zero order [21]. Finally, The expected value of throughput corresponding to Mode I conditioned on  $\mathbf{h}_k$  can be written as

$$\begin{aligned} & \mathbb{E}[T_{k+1,1}(\gamma)] \\ &= \int_0^\infty T\left(\frac{y}{N_0}\right) \cdot \frac{1}{1-\rho} \exp\left(\frac{-(y + \rho |\mathbf{h}_k^H \mathbf{f}_k^s|^2)}{1-\rho}\right) \cdot I_0\left(\frac{2}{1-\rho} \sqrt{\rho y |\mathbf{h}_k^H \mathbf{f}_k^s|^2}\right) dy \end{aligned} \quad (3.16)$$

The derivation given above is based on the assumption that the channel correlation  $\rho$  is not equal to 1, or Equation (3.12) does not make any sense. In this case, when  $\rho$  is equal to 1, the channel condition of the  $k$ th frame is the same to that of the  $(k+1)$ th frame, so the expectation is meaningless and the throughput of the  $(k+1)$ th frame is the same to that of the  $k$ th frame.



### 3.3.2 Computation of Modal Metric in Mode II

The expected value of throughput corresponding to Mode II is much involved than that in Mode I since the best precoder is reselected in the  $(k+1)$ th frame. Therefore, we have two uncertainties:  $\mathbf{h}_{k+1}^H$  and  $\mathbf{f}_{k+1}$ . The formula for the expected value of throughput is formulated in the same way to that under Mode I

$$\mathbb{E}[T_{k+1,2}(\gamma)] = \int_0^\infty T_{k+1,2}(\gamma) \cdot f_\Gamma(\gamma | \mathbf{h}_k) d\gamma \quad (3.17)$$

The receive SNR can then be derived as

$$\begin{aligned} \Gamma &= \text{SNR} \cdot \left| \mathbf{h}_{k+1}^H \mathbf{f}_{k+1}^s \right|^2 \\ &= \text{SNR} \cdot \left\| \mathbf{h}_{k+1} \right\|^2 \cdot \max_{\mathbf{f}_i \in \mathcal{F}_2} \left| \frac{\mathbf{h}_{k+1}^H}{\left\| \mathbf{h}_{k+1} \right\|} \mathbf{f}_i \right|^2 \\ &= \text{SNR} \cdot U \cdot \widehat{V} \end{aligned} \quad (3.18)$$

where  $U = \left\| \mathbf{h}_{k+1} \right\|^2$ ,  $\widehat{V} = \max_{\mathbf{f}_i \in \mathcal{F}_2} \left| \frac{\mathbf{h}_{k+1}^H}{\left\| \mathbf{h}_{k+1} \right\|} \mathbf{f}_i \right|^2$ . In other words, the receive SNR is a

multiplication of two random variables  $U$  and  $\widehat{V}$  under the condition that  $\mathbf{h}_k$  is given.

The derivation of PDF of  $U$  conditioned on  $\mathbf{h}_k$  is similar to that of  $Y$  in Mode I, so we omit it here. The result is

$$f_U(u | \mathbf{h}_k) = \frac{2}{1-\rho} f_W\left(\frac{2u}{1-\rho}\right) \quad (3.19)$$

where the random variable  $W$  is noncentral chi-square distributed with  $2N_t$  degrees of freedom and non-centrality parameter  $\lambda$  being  $2\rho \left\| \mathbf{h}_k \right\|^2 / (1-\rho)$ .

The PDF of the random variable  $\widehat{V}$  also depends on  $\mathbf{h}_k$  and is difficult to obtain. Therefore, in [11], the PDF of the random variable  $\widehat{V}$  is replaced by an upper

bound, thus the resulted expected value is a lower bound, which is questionable to be used as a modal metric in Mode selection. Therefore, in our work, we turn to use  $V$ , which is a random variable generated from  $\hat{V}$  with  $\mathbf{h}_k$  being averaged out, as our alternative. With the help of numerical experiments, the plot of  $f_V(v)$  is depicted in Fig. 3-2. Then we approximate the PDF of random variable  $V$  with Gamma distribution [22, 23]

$$f(v) = v^{a-1} \frac{\exp(-v/b)}{\Gamma(a) \cdot b^a} \quad v \in [0, \infty) \quad (3.20)$$

where  $\kappa = 26.5$  and  $\eta = 0.023$ . Although the support of gamma distribution lies in  $\mathbb{R}^+$ , which does not match that of random variable  $V$ , we may still regard  $f(v)$  as an approximation of the distribution of  $V$ , thus

$$f_V(v) \cong v^{\kappa-1} \frac{\exp(-v/\eta)}{\Gamma(\kappa) \cdot \eta^\kappa} \quad x \in [0, 1] \quad (3.21)$$

To examine the tightness of this approximation, we compare the root mean square error (RMSE) of using the function  $f(v)$  as well as that of using different order of polynomials, and the result is plotted in Fig. 3-3. As we can see, the approximation with  $f(v)$  is tight enough.

Moreover, two random variables  $U$  and  $V$  are independent. Instead of giving a proof in detail, we provide an alternative way to demonstrate it. The chief reason for the independence lies in the fact that  $V$  has nothing do with  $\mathbf{h}_k$ , thus making them an independent pair. To better illustrate this, we give the graphs of the jointly distribution of  $UV$  and the product of their distributions.

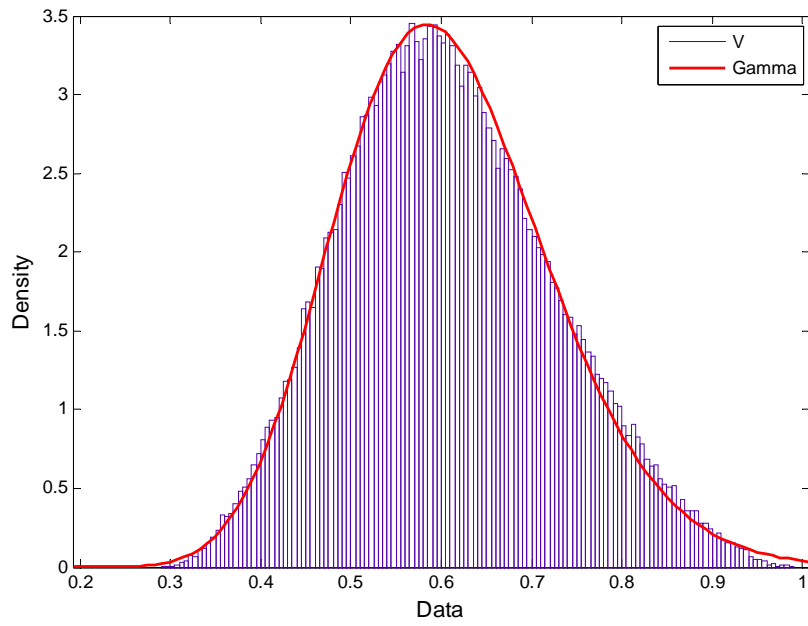


Fig. 3-2 Histogram of the random variable  $V$  and its approximation with Gamma distribution

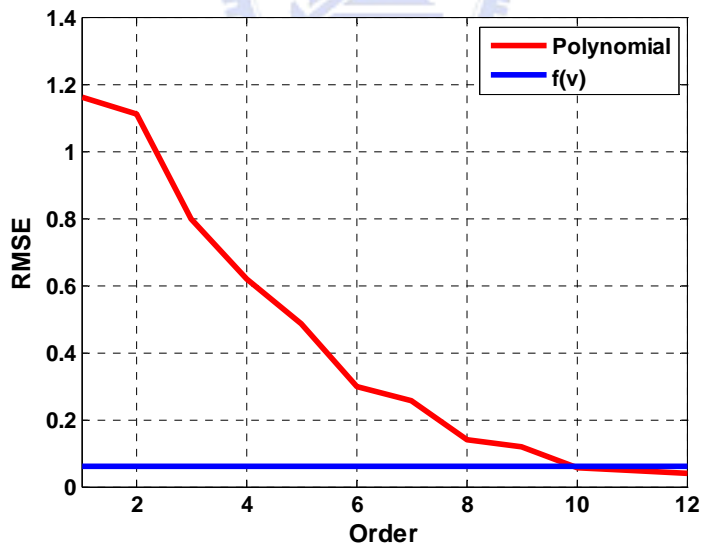


Fig. 3-3 The RMSE of using  $f(v)$  and using different order of polynomials

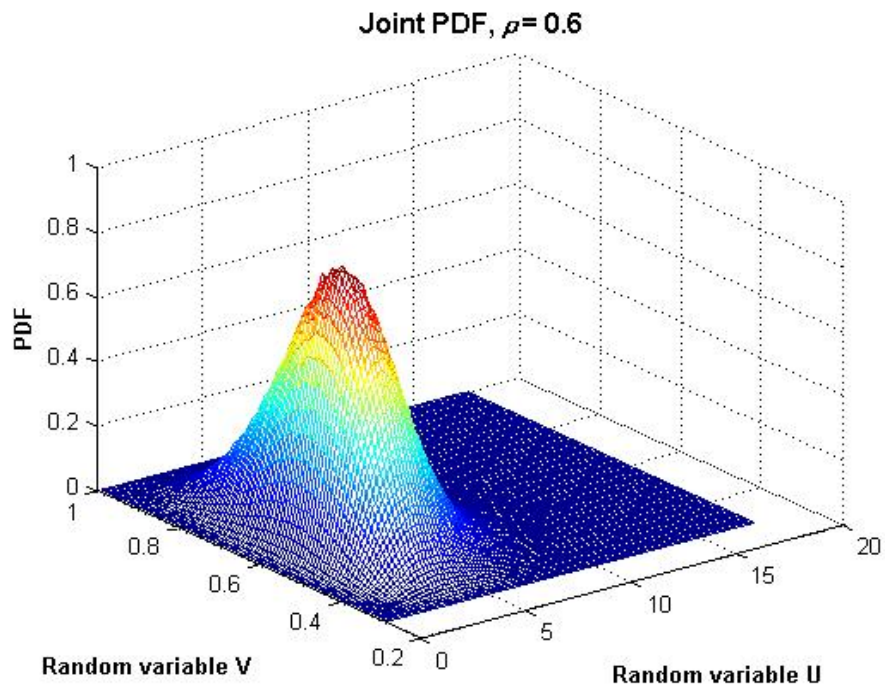


Fig. 3-4 Joint PDF of random variables  $V$  and  $U$

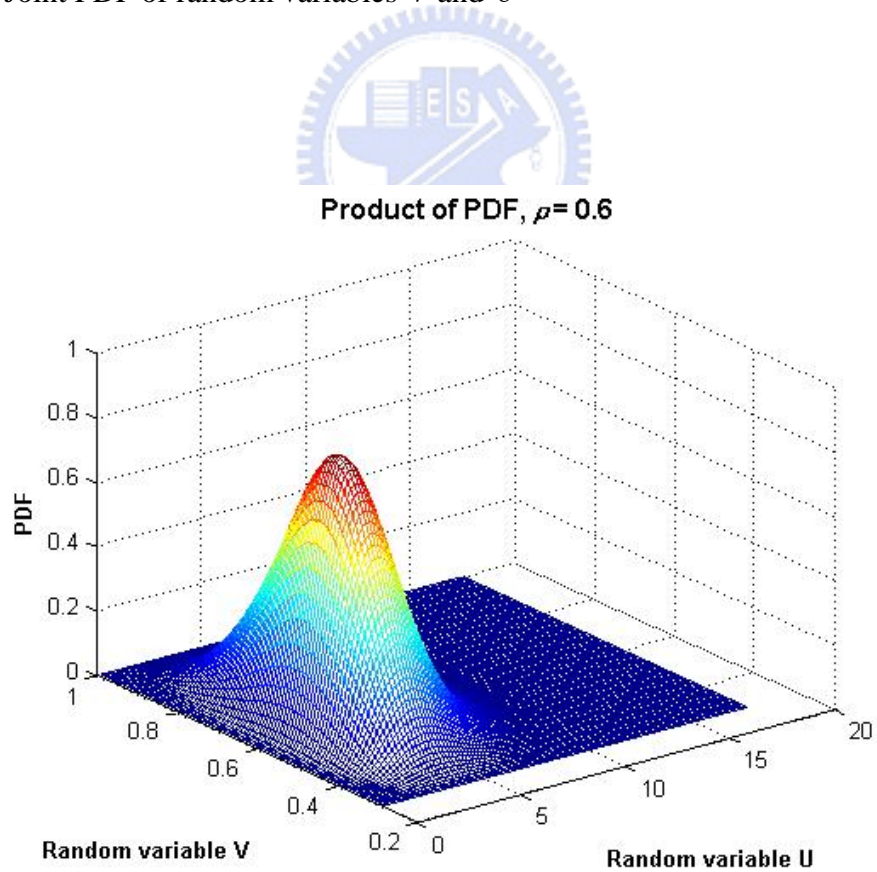


Fig. 3-5 Product of PDFs of random variables  $V$  and  $U$

### 3.4 Selection of Good Mode and Beamformer

The rule for selecting a suitable mode and a specific precoder is described as follows: the receiver first determines the mode  $m$  for use based on the value of each modal metric, i.e., Mode I is chosen if  $\Gamma_1 > \Gamma_2$  and Mode II on the other hand.

$$\begin{cases} m = 1 \text{ (Mode I)} & , \text{ if } \Gamma_1 > \Gamma_2 \\ m = 2 \text{ (Mode II)} & , \text{ if } \Gamma_2 > \Gamma_1 \end{cases} \quad (3.22)$$

After choosing the mode type, the receiver chooses the precoder  $\mathbf{f}^s$  maximizing the throughput

$$\mathbf{f}^s = \arg \max_{\mathbf{f} \in \mathcal{F}_m} T(\gamma) \quad m \in \{1, 2\} \quad (3.23)$$

and feeds back the index of the precoder to the transmitter. Since  $T(\gamma)$  is a monotonically increasing function of  $\gamma$ , (3.23) becomes

$$\mathbf{f}^s = \arg \max_{\mathbf{f}_k \in \mathcal{F}_m} |\mathbf{h}_k^H \mathbf{f}_k|^2 \quad m \in \{1, 2\} \quad (3.24)$$

The rule for selecting a good mode and a beamformer can be better described in the following flow chart.

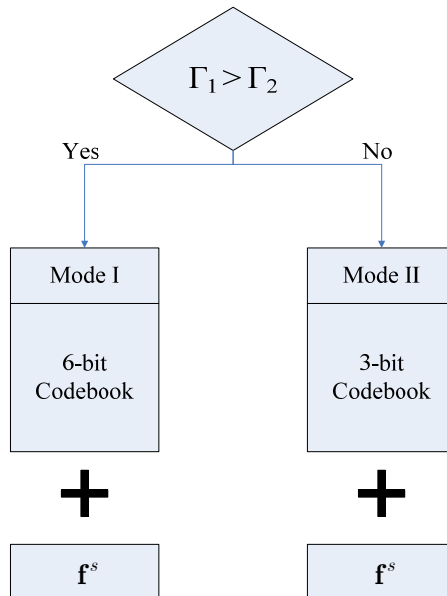


Fig. 3-6 Flow chart of selecting a mode and a beamformer

### 3.5 Numerical Results

In this section, we shall give some simulations to demonstrate the advantages of the dual-mode scheme and the proposed selection criterion. Table 3-1 lists all parameters in our simulation.

Table 3-1 Simulation parameters

<b>Parameter</b>	<b>Value</b>
<b>Channel</b>	Rayleigh fading channel (First-order Markov channel model)
<b>Modulation</b>	16 QAM
<b>Number of transmit antennas</b>	4
<b>Number of receive antennas</b>	1
<b>Fixed average feedback rate</b>	3 bits per frame
<b>Frame length</b>	128 symbols
<b>Number of frames</b>	10000
<b>Codebook</b>	Transmit beamforming codebooks in IEEE 802.16-2005

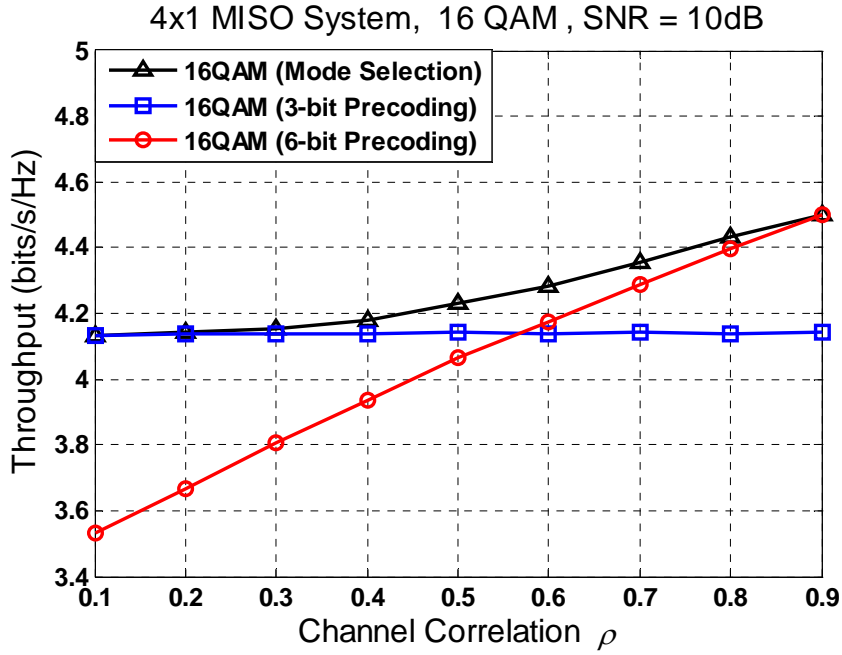


Fig. 3-7 Dual-mode scheme and single-mode scheme with SNR = 10dB and 16 QAM

In this figure, we can observe that the dual-mode scheme with the proposed mode selection criterion adequately switch between the other two single-mode schemes, which in our case are the 3-bit precoding scheme and the 6-bit precoding scheme. In low-correlation regime, the receiver prefers Mode II. Due to the rapid fluctuation of channel statistics, the system is able to achieve better performance if it reselects the precoder at the start of each frame. On the other hand, in high-correlation regime, the receiver turns to use Mode I. Because the channel statistics varies slowly, the high resolution of the 6-bit codebook is able to compensate for the performance degradation due to the use of same precoder over two frames.

Moreover, the dual-mode scheme outperforms both other single-mode schemes in the middle range of channel correlations. In particular, at  $\rho = 0.6$ , there is an improvement of performance of 0.2 bits/s/Hz, and the gap vanishes with the increase or decrease of channel correlation. The reason is that the larger the channel correlation becomes, the more likely Mode I is adopted; the smaller the channel correlation becomes, the more likely Mode II is adopted.

## 3.6 Summary

In this chapter, we first introduce the dual-mode scheme in which two different sizes of codebooks are adopted. The goal of using dual-mode scheme is to achieve a better system performance on the premise that adequate selection criterion can be used to switch between the two. Afterwards, we propose our mode selection criterion by first defining the throughput in this work and then the modal metric.

In Section 3.2, we give the definition of the throughput whose physical meaning is the number of correct bits per second that can be achieved without any error-control coding if the transmitter use the channel capacity as the transmission rate. In Section 3.3, the definition of the modal metric is given. The modal metric is able to exploit the channel correlation between the consecutive two frames by taking average of the throughputs corresponding to each mode under the assumption that the receiver has full knowledge CSI. In particular, the modal metric involves the expectation of the throughput pertaining to the next frame since the receiver has no idea about the exact channel condition of it. The detailed analysis of modal metric corresponding to Mode I and Mode II is also derived. Then in Section 3.4, we describe the selection rule for the good mode and the precoder. Finally, a simulation is given to justify the proposed algorithm for the dual-mode scheme.



# Chapter 4

## Modal Metric Approximation

In Chapter 3, the definition and derivation of the modal metric corresponding to Mode I and Mode II are given; moreover, simulations justify the utility of the modal metric by showing that the dual-mode scheme outperforms the single-mode scheme over full range of channel correlations. The superior performance is ascribed to the consideration of channel correlation in the modal metric. Namely, the expected value of throughput of the coming frame is considered when performing the mode selection.

While the expected value of the throughput with respect to Mode I and Mode II are derived in Chapter 3, the integrals are a little bit troublesome when performing this algorithm in practical, and to simplify the computation of this integral is one of the future works in [11]. Therefore, we wonder if there are closed-form solutions for them. Unfortunately, to our best knowledge, due to the combination of the various difficult-analyzing functions in the integrals, the answer is no. To seek what is less attractive than our original objective, we try to find the approximations for them.

In this chapter, we shall analyze Equation (3.10) and (3.17) as well as derive the approximations for them respectively. Then, some numerical results will be given to demonstrate the accuracy of the approximations.

## 4.1 Approximation of Modal Metric in Mode I

We start the approximation with the equation (3.10) and assume that  $\rho \neq 1$ .

Since (3.10) can be rewritten as

$$\int_0^\infty T\left(\frac{y}{N_0}\right) \cdot \frac{1}{a} f_Z\left(\frac{y}{a}\right) dy. \quad (4.1)$$

We first analyze  $f_Z(y/a)/a$ . Recall that  $a = (1 - \rho)/2$  and

$$f_Z(z) = \frac{1}{2} \exp\left(\frac{-(z + \lambda)}{2}\right) \cdot I_0(\sqrt{\lambda z}) \quad (4.2)$$

where

$$\lambda = \frac{2}{1 - \rho} \left| \sqrt{\rho} \mathbf{h}_k^H \mathbf{f}_k^s \right|^2 \quad (4.3)$$

therefore

$$\begin{aligned} \frac{1}{a} f_Z\left(\frac{y}{a}\right) &= \frac{1}{1 - \rho} \exp\left(\frac{-\left(\frac{2y}{1 - \rho} + \frac{2\rho}{1 - \rho} \left| \mathbf{h}_k^H \mathbf{f}_k^s \right|^2\right)}{2}\right) \cdot I_0\left(\sqrt{\frac{2\rho}{1 - \rho} \left| \mathbf{h}_k^H \mathbf{f}_k^s \right|^2 \frac{2y}{1 - \rho}}\right) \\ &= R_1\left(\rho, \left| \mathbf{h}_k^H \mathbf{f}_k^s \right|^2\right) \cdot \exp\left(\frac{-y}{1 - \rho}\right) \cdot I_0\left(\frac{2}{1 - \rho} \sqrt{\rho y \left| \mathbf{h}_k^H \mathbf{f}_k^s \right|^2}\right) \end{aligned} \quad (4.4)$$

where

$$R_1\left(\rho, \left| \mathbf{h}_k^H \mathbf{f}_k^s \right|^2\right) = \frac{1}{1 - \rho} \exp\left(\frac{-\rho \left| \mathbf{h}_k^H \mathbf{f}_k^s \right|^2}{1 - \rho}\right) \quad (4.5)$$

Therefore (4.1) turns to

$$\begin{aligned} \int_0^\infty T\left(\frac{y}{N_0}\right) \cdot \frac{1}{a} f_Z\left(\frac{y}{a}\right) dy &= R_1\left(\rho, \left| \mathbf{h}_k^H \mathbf{f}_k^s \right|^2\right) \\ &\cdot \int_0^\infty \left[ \log_2\left(1 + \frac{y}{N_0}\right) \cdot \left(1 - 2\left(1 - \frac{1}{\sqrt{M}}\right) Q\left(\sqrt{\frac{3}{M - 1} \frac{y}{N_0}}\right)\right)^2 \cdot \exp\left(\frac{-y}{1 - \rho}\right) \cdot I_0\left(\frac{2}{1 - \rho} \sqrt{\rho y \left| \mathbf{h}_k^H \mathbf{f}_k^s \right|^2}\right) \right] dy \end{aligned} \quad (4.6)$$

Since Q-function has no closed form representation, we turn to its approximation

[24]:

$$Q(x) \cong \frac{1}{12} \exp\left(-\frac{x^2}{2}\right) + \frac{1}{4} \exp\left(-\frac{2x^2}{3}\right) \quad (4.7)$$

With this approximation,

$$\begin{aligned} & \left(1 - 2\left(1 - \frac{1}{\sqrt{M}}\right)Q\left(\sqrt{\frac{3}{M-1} \frac{y}{N_0}}\right)\right)^2 \\ &= \left(1 - 2\left(1 - \frac{1}{\sqrt{M}}\right)\left[\frac{1}{12} \exp\left(-\frac{3}{2(M-1)} \frac{y}{N_0}\right) + \frac{1}{4} \exp\left(-\frac{2}{M-1} \frac{y}{N_0}\right)\right]\right)^2 \\ &= 1 - \frac{\sqrt{M}-1}{3\sqrt{M}} \exp\left(-\frac{3}{2(M-1)} \frac{y}{N_0}\right) - \frac{\sqrt{M}-1}{\sqrt{M}} \exp\left(-\frac{2}{M-1} \frac{y}{N_0}\right) \\ &+ 4\left(\frac{M-2\sqrt{M}+1}{M}\right) \left[\frac{1}{144} \exp\left(-\frac{3}{(M-1)} \frac{y}{N_0}\right) + \frac{1}{24} \exp\left(-\frac{7}{2(M-1)} \frac{y}{N_0}\right)\right] \\ &+ \frac{1}{16} \exp\left(-\frac{4}{M-1} \frac{y}{N_0}\right) \end{aligned} \quad (4.8)$$

Denote by  $E(\alpha, \beta)$  the integral

$$\begin{aligned} & R_1\left(\rho, \left|\mathbf{h}_k^H \mathbf{f}_k^s\right|^2\right) \cdot \\ & \int_0^\infty \left[\log_2\left(1 + \frac{y}{N_0}\right) \cdot \alpha \exp\left(-\beta \frac{y}{N_0}\right) \cdot \exp\left(\frac{-y}{1-\rho}\right) \cdot I_0\left(\frac{2}{1-\rho} \sqrt{\rho y \left|\mathbf{h}_k^H \mathbf{f}_k^s\right|^2}\right)\right] dy \end{aligned} \quad (4.9)$$

Equation (4.6) turns to

$$\begin{aligned} & \left[ E(1, 0) - E\left(\frac{\sqrt{M}-1}{3\sqrt{M}}, \frac{3}{2(M-1)}\right) \right. \\ & \left. - E\left(\frac{\sqrt{M}-1}{\sqrt{M}}, \frac{2}{M-1}\right) + E\left(\frac{1}{36} \left(\frac{M-2\sqrt{M}+1}{M}\right), \frac{3}{(M-1)}\right) \right. \\ & \left. + E\left(\frac{1}{6} \left(\frac{M-2\sqrt{M}+1}{M}\right), \frac{7}{2(M-1)}\right) + E\left(\frac{1}{4} \left(\frac{M-2\sqrt{M}+1}{M}\right), \frac{4}{M-1}\right) \right] \end{aligned} \quad (4.10)$$

Unfortunately, to our best knowledge (4.9) has no closed-form representation. To approximate it, we first try to replace the log function in the integrand with elementary functions so that other known integral formula can be applied. Due to the existence of exponential function, the integrand decays very fast and is negligible for  $x > 20$ , so we approximate the log function with a polynomial using least squares

fitting [25]:

$$\log_2 \left( 1 + \frac{y}{N_0} \right) \cong \sum_{n=0}^7 a_n y^n \quad y \in [0, 20]. \quad (4.11)$$

Therefore, (4.9) becomes

$$E(\alpha, \beta) \cong R_1 \left( \rho, |\mathbf{h}_k^H \mathbf{f}_k^s|^2 \right) \cdot \alpha \sum_{n=0}^7 a_n \int_0^\infty y^n \exp \left[ - \left( \frac{\beta}{N_0} + \frac{1}{1-\rho} \right) y \right] \cdot I_0 \left( \frac{2}{1-\rho} \sqrt{\rho y |\mathbf{h}_k^H \mathbf{f}_k^s|^2} \right) dy. \quad (4.12)$$

Let  $\hat{y} = y\rho |\mathbf{h}_k^H \mathbf{f}_k^s|^2$ , then

$$E(\alpha, \beta) \cong \alpha R_1 \left( \rho, |\mathbf{h}_k^H \mathbf{f}_k^s|^2 \right) \cdot \sum_{n=0}^7 \frac{a_n}{\rho^{n+1} |\mathbf{h}_k^H \mathbf{f}_k^s|^{2(n+1)}} \cdot \int_0^\infty \exp \left[ - \left( \frac{\beta}{N_0} + \frac{1}{1-\rho} \right) \frac{\hat{y}}{\rho |\mathbf{h}_k^H \mathbf{f}_k^s|^2} \right] \cdot I_0 \left( \frac{2}{1-\rho} \sqrt{\hat{y}} \right) d\hat{y} \quad (4.13)$$

At this point, Let us postpone the computation of this integral for a moment and consider the following lemmas in [21]:

*Lemma 1*

$$\begin{aligned} & \int_0^\infty x^{a-\frac{1}{2}} \exp(-Ax) I_{2b}(2B\sqrt{x}) dx \\ &= \frac{\Gamma \left( a + b + \frac{1}{2} \right)}{\Gamma(2b+1)} B^{-1} \exp \left( \frac{B^2}{2A} \right) A^{-a} M_{-a,b} \left( \frac{B^2}{A} \right) \quad \text{Re} \left( a + b + \frac{1}{2} \right) > 0 \end{aligned} \quad (4.14)$$

where  $M_{a,b}(\cdot)$  is Whittaker function [21].

*Lemma 2*

$$M_{a,b}(x) = x^{b+\frac{1}{2}} \exp \left( -\frac{x}{2} \right) \Phi \left( b - a + \frac{1}{2}, 2b + 1; x \right) \quad (4.15)$$

$\Phi(\cdot)$  is confluent hypergeometric function [21].

With *Lemma 1* and *Lemma 2*, (4.13) becomes

$$E(\alpha, \beta) \cong \alpha R_1 \left( \rho, |\mathbf{h}_k^H \mathbf{f}_k^s|^2 \right) \cdot \sum_{n=0}^7 a_n \cdot \Gamma(n+1) C^{-(n+1)} \Phi \left( n+1, 1; \frac{B^2}{A} \right) \quad (4.16)$$

where  $A = \left( \frac{\beta}{N_0} + \frac{1}{1-\rho} \right) \cdot \frac{1}{\rho |\mathbf{h}_k^H \mathbf{f}_k^s|^2}$ ,  $C = \left( \frac{\beta}{N_0} + \frac{1}{1-\rho} \right)$  and  $B = \frac{1}{1-\rho}$ .

To compute  $\Phi(n+1, 1; B^2/A)$ , we again use the following lemmas in [21]:

*Lemma 3*

$$\Phi(p, p; x) = e^x \quad (4.17)$$

*Lemma 4*

$$\Phi(p, q; x) = \frac{(x+2p-2-q)}{p-1} \Phi(p-1, q; x) + \frac{(q-p+1)}{p-1} \Phi(p-2, q; x) \quad (4.18)$$

*Lemma 5*

$$M_{n+b+\frac{1}{2}, b}^{(x)} = \frac{x^{\frac{1}{2}-b} e^{\frac{1}{2}x}}{(2b+1)(2b+2)\cdots(2b+n)} \frac{d^n}{dx^n} (x^{n+2b} e^{-x}) \quad (4.19)$$

with  $n = 0, 1, 2, \dots$  and  $2b \neq -1, -2, -3, \dots$

*Lemma 6*

$$x^{\frac{1}{2}-b} M_{a,b}^{(x)} = (-x)^{\frac{1}{2}-b} M_{-a,b}^{(-x)} \quad (4.20)$$

with  $2b \neq -1, -2, -3, \dots$

Therefore, with *Lemma 2* to *Lemma 6*, we obtain the following results:

$$\Phi(1, 1; x) = e^x \quad (4.21)$$

$$\Phi(2, 1; x) = e^x (1+x) \quad (4.22)$$

$$\Phi(n, 1; x) = \frac{(x+2n-3)}{n-1} \Phi(n-1, 1; x) + \frac{(2-n)}{n-1} \Phi(n-2, 1; x) \quad , n \geq 2 \quad (4.23)$$

## 4.2 Approximation of Modal Metric in Mode II

Assuming  $\rho \neq 1$  and putting (3.21) and (3.19) into (3.17), we obtain

$$\mathbb{E}[T_{k+1,2}(\gamma)] \cong \int_{u=0}^{\infty} \int_{v=0}^1 T(\text{SNR} \cdot uv) \cdot \frac{1}{a} f_W\left(\frac{u}{a} \mid \mathbf{h}_k, \rho\right) \cdot v^{\kappa-1} \frac{\exp(-v/\eta)}{\Gamma(\kappa) \cdot \eta^{\kappa}} dv du \quad (4.24)$$

where  $\kappa = 26.5, \eta = 0.023$ , and  $a = (1 - \rho) / 2$ .

For simplicity, we denote (4.24) as

$$\int_{u=0}^{\infty} H(u) du \quad (4.25)$$

where

$$H(u) = \int_{v=0}^1 T(\text{SNR} \cdot uv) \cdot \frac{1}{a} f_W\left(\frac{u}{a} \mid \mathbf{h}_k, \rho\right) \cdot v^{\kappa-1} \frac{\exp(-v/\eta)}{\Gamma(\kappa) \cdot \eta^{\kappa}} dv \quad (4.26)$$

Since the random variable  $W$  is noncentral chi-square distributed with  $2N_t$  degrees of freedom and the non-centrality parameter  $\lambda$  being  $2\rho \|\mathbf{h}_k\|^2 / (1 - \rho)$ ,

(4.26) can then be rewritten as

$$\begin{aligned} H(u) &= \frac{1}{\Gamma(\kappa) \cdot \eta^{\kappa}} \cdot R_2\left(\rho, \|\mathbf{h}_k\|^2, N_t\right) \cdot \exp\left(\frac{-u}{1-\rho}\right) \cdot (u)^{\frac{N_t-1}{2}} \\ &\cdot I_{N_t-1}\left(\frac{2}{1-\rho} \sqrt{\rho u \|\mathbf{h}_k\|^2}\right) \cdot \left(\frac{1}{\rho \|\mathbf{h}_k\|^2}\right)^{\frac{N_t-1}{2}} \\ &\cdot \int_{v=0}^1 \left[ \log_2\left(1 + \frac{uv}{N_0}\right) \cdot \left(1 - 2\left(1 - \frac{1}{\sqrt{M}}\right) Q\left(\sqrt{\frac{3}{M-1} \frac{uv}{N_0}}\right)\right)^2 \right] \cdot v^{\kappa-1} \exp(-v/\eta) dv \end{aligned} \quad (4.27)$$

where

$$R_2\left(\rho, \|\mathbf{h}_k\|^2, N_t\right) = \frac{1}{1-\rho} \exp\left(\frac{-(\rho \|\mathbf{h}_k\|^2)}{1-\rho}\right) \quad (4.28)$$

Again, we use the approximation in (4.7) for Q-function, so

$$\begin{aligned}
H(u) &\cong \\
&R_2\left(\rho, \|\mathbf{h}_k\|^2, N_t\right) \cdot \exp\left(\frac{-u}{1-\rho}\right) \cdot (u)^{\frac{N_t-1}{2}} \\
&\cdot I_{N_t-1}\left(\frac{2}{1-\rho} \sqrt{\rho u \|\mathbf{h}_k\|^2}\right) \cdot \left(\frac{1}{\rho \|\mathbf{h}_k\|^2}\right)^{\frac{N_t-1}{2}} \\
&\left[ D(u, 1, 0) - D\left(u, \frac{\sqrt{M}-1}{3\sqrt{M}}, \frac{3}{2(M-1)}\right) - D\left(u, \frac{\sqrt{M}-1}{\sqrt{M}}, \frac{2}{M-1}\right) \right. \\
&+ D\left(u, \frac{1}{36} \left(\frac{M-2\sqrt{M}+1}{M}\right), \frac{3}{M-1}\right) \\
&+ D\left(u, \frac{1}{6} \left(\frac{M-2\sqrt{M}+1}{M}\right), \frac{7}{2(M-1)}\right) \\
&\left. + D\left(u, \frac{1}{4} \left(\frac{M-2\sqrt{M}+1}{M}\right), \frac{4}{M-1}\right) \right] \quad (4.29)
\end{aligned}$$

where

$$\begin{aligned}
&D(u, \alpha, \beta) \\
&= \frac{1}{\Gamma(\kappa) \cdot \eta^\kappa} \cdot \int_{v=0}^1 \left[ \log_2 \left( 1 + \frac{uv}{N_0} \right) \cdot \alpha \exp\left(-\beta \frac{uv}{N_0}\right) \cdot v^{\kappa-1} \exp(-v/\eta) \right] dv \quad (4.30)
\end{aligned}$$

With numerical experiment, we find that  $H(u)$  decays very fast and is negligible for  $x > 20$ , so we approximate  $D(u, \alpha, \beta)$  with a polynomial  $f(u, \alpha, \beta)$  using least squares fitting [25]:

$$f(u, \alpha, \beta) = \sum_{n=0}^7 a_n u^n \quad u \in [0, 20]. \quad (4.31)$$

Denote  $F(\alpha, \beta)$  by

$$\begin{aligned}
&R_2\left(\rho, \|\mathbf{h}_k\|^2, N_t\right) \cdot \left(\frac{1}{\rho \|\mathbf{h}_k\|^2}\right)^{\frac{N_t-1}{2}} \\
&\cdot \int_0^\infty \exp\left(\frac{-u}{1-\rho}\right) \cdot (u)^{\frac{N_t-1}{2}} \cdot I_{N_t-1}\left(\frac{2}{1-\rho} \sqrt{\rho u \|\mathbf{h}_k\|^2}\right) \cdot f(u, \alpha, \beta) du \quad (4.32)
\end{aligned}$$

then

$$\begin{aligned}
\mathbb{E}[T_{k+1,2}(\gamma)] &\cong \\
&F(1,0) - F\left(\frac{\sqrt{M}-1}{3\sqrt{M}}, \frac{3}{2(M-1)}\right) - F\left(\frac{\sqrt{M}-1}{\sqrt{M}}, \frac{2}{M-1}\right) \\
&+ F\left(\frac{1}{36}\left(\frac{M-2\sqrt{M}+1}{M}\right), \frac{3}{M-1}\right) + F\left(\frac{1}{6}\left(\frac{M-2\sqrt{M}+1}{M}\right), \frac{7}{2(M-1)}\right) \\
&+ F\left(\frac{1}{4}\left(\frac{M-2\sqrt{M}+1}{M}\right), \frac{4}{M-1}\right)
\end{aligned} \tag{4.33}$$

The computation for  $F(\alpha, \beta)$  is similar to that for (4.12), and the result is

$$\begin{aligned}
F(\alpha, \beta) &= \exp\left(\frac{-(\rho\|\mathbf{h}_k\|^2)}{1-\rho}\right) \\
&\cdot \left[ \sum_{n=0}^7 a_n \frac{\Gamma(N_t+n)}{\Gamma(N_t)} B^{-n} \Phi\left(N_t+n, N_t; \frac{B^2}{A}\right) \right]
\end{aligned} \tag{4.34}$$

where  $A = \frac{1}{\rho(1-\rho)\|\mathbf{h}_k\|^2}$ , and  $B = \frac{1}{1-\rho}$ . The closed form representation for

$\Phi(\cdot)$  can be obtained with *Lemma 2* to *Lemma 6*.





## 4.3 Numerical Results

In this section, we give some simulation results to demonstrate the effectiveness of the throughput-based criterion. For the sake of simplicity, we denote  $\mathbb{E}[T_{k+1,1}(\gamma)]$  as  $T_1$ ; approximated  $\mathbb{E}[T_{k+1,1}(\gamma)]$  as  $T_1^*$ ;  $\mathbb{E}[T_{k+1,2}(\gamma)]$  as  $T_2$ ; approximated  $\mathbb{E}[T_{k+1,2}(\gamma)]$  as  $T_2^*$ . Moreover, the throughput performance with respect to the dual-mode scheme, the single-mode scheme with 3-bit precoding, and the single-mode scheme with 6-bit precoding are also given. Finally the proposed mode selection criterion is compared with other criteria. Table 4-1 lists all parameters in our simulations.

Table 4-1 Simulation parameters

Parameter	Value
Channel	Rayleigh fading channel (First-order Markov channel model)
Modulation	16QAM, 64 QAM
Number of transmit antennas	4
Number of receive antennas	1
Fixed average feedback rate	3 bits per frame
Frame length	128 symbols
Number of frames	10000
Codebook	Transmit beamforming codebooks in IEEE 802.16-2005
Selection criteria	Throughput-based criterion, SER-based criterion, and randomly-selecting criterion

### 4.3.1 Approximation vs. Exact Value (Mode I)

Fig. 4-1 shows the expected value of throughput over the  $(k + 1)$ th frame under Mode I with 16-QAM modulation. Three different channel correlations:  $\rho = 0.1$ ,  $\rho = 0.5$ , and  $\rho = 0.9$  are considered. First, the expected value of the throughput over the  $(k + 1)$ th frame is an increasing function of SNR. Second, As the channel correlation gets larger, the performance gets better. The reason is that the best precoder for beamforming over the  $k$ th frame is near optimal for the  $(k + 1)$ th frame. Moreover, the approximation of the expected value is shown to be very tight for different channel correlations and SNRs. The proposed approximation is also shown to be very tight for different modulations in Fig. 4-2

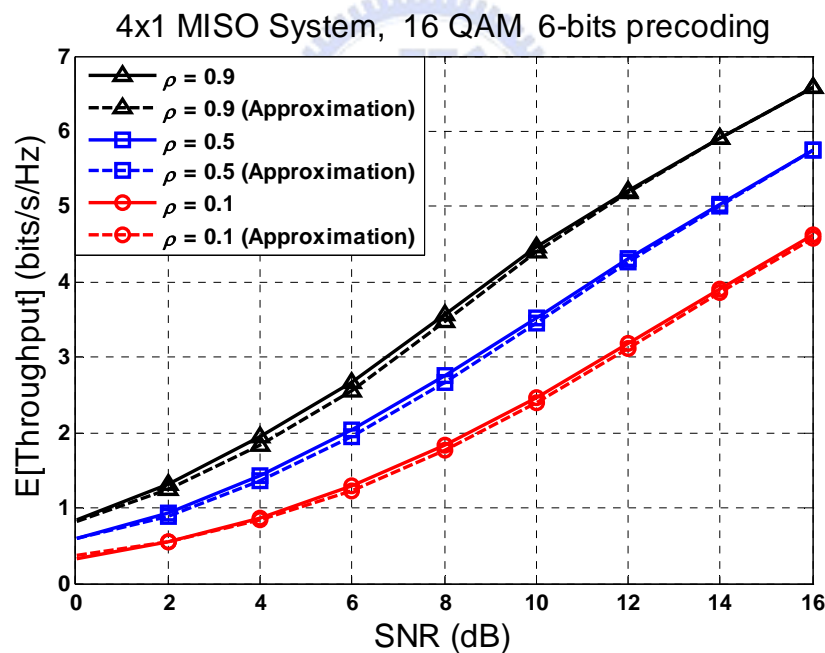


Fig. 4-1  $T_1$  vs.  $T_1^*$  with 16 QAM and different channel correlations

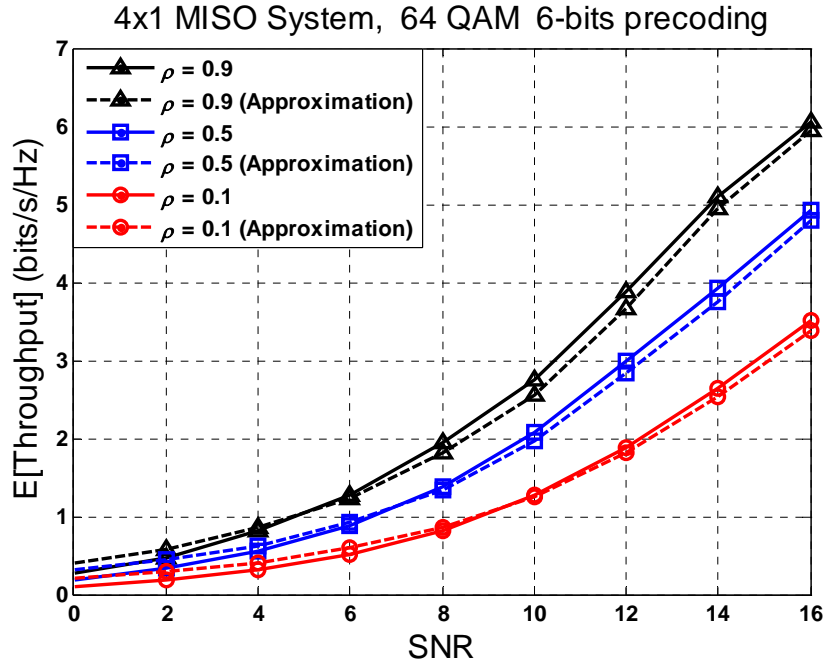


Fig. 4-2  $T_1$  vs.  $T_1^*$  with 64 QAM and different channel correlations

### 4.3.2 Approximation vs. Exact Value (Mode II)

Fig. 4-3 shows the expected value of throughput over the  $(k + 1)$  th frame under Mode II with 16-QAM modulation. Three different channel correlations:  $\rho = 0.1$ ,  $\rho = 0.5$ , and  $\rho = 0.9$  are considered. First, the expected value of the throughput over the  $(k + 1)$  th frame is an increasing function of SNR. Second, we can observe that unlike Mode I, in which the performance gets better as the channel correlation gets larger, the performance corresponding to different channel correlations are almost the same. The reason is that the best precoder for beamforming over the  $k$  th frame is reselected for the  $(k + 1)$  th frame, so the expected value of the throughput has nothing to do with channel correlation, and this can be also realized by Equation (4.34). Moreover, the approximation of the expected value is shown to be very tight for different channel correlations and SNRs. Also, the proposed approximation is also shown to be very tight for different modulations in Fig. 4-4.

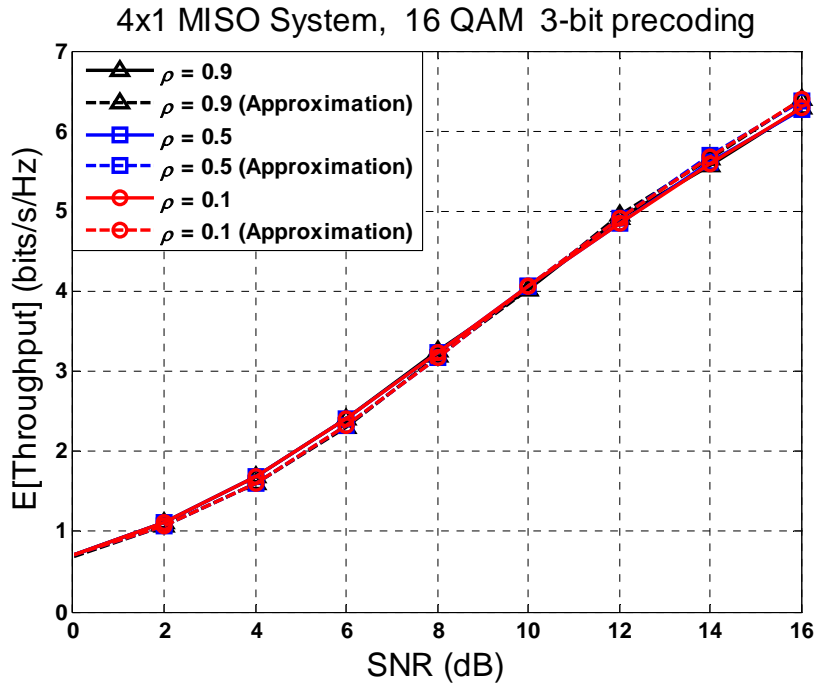


Fig. 4-3  $T_2$  vs.  $T_2^*$  with 16 QAM and different channel correlations

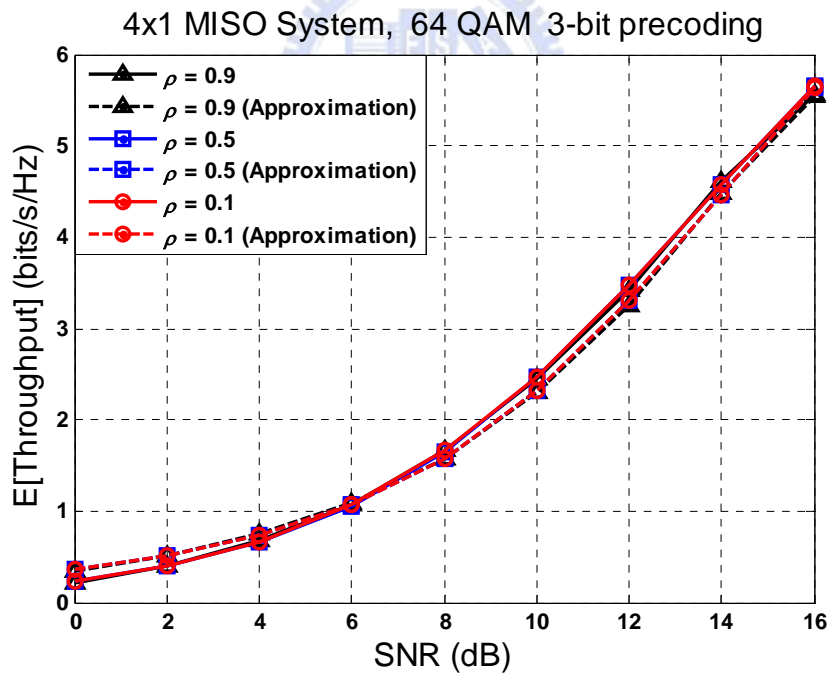


Fig. 4-4  $T_2$  vs.  $T_2^*$  with 64 QAM and different channel correlations

### 4.3.3 Dual-Mode Scheme vs. Single-Mode Scheme

To better examine the improvement of the dual-mode scheme over the single-mode scheme, average throughput over different channel correlations at a fixed transmit SNR is compared. In Fig. 4-5 and Fig. 4-6, each figure has four lines corresponding to the single-mode schemes with 3-bit and 6-bit codebook respectively, the dual-mode scheme using exact modal metric, and the dual-mode scheme using the approximated modal metric.

In each figure, we can see that the system performance does not remain well in all channel correlations using Mode I or Mode II exclusively. Mode I is good at low channel correlations since the receiver selects the best precoder at each time frame. While at high channel correlations, Mode II works better since the high resolution of the codebook compensates for the loss caused by choosing precoder seldom. Finally, the proposed algorithm of model selection works well for the dual-mode scheme which outperforms each single-mode scheme in full range of channel correlations because it always selects a better mode for use. Moreover, the proposed approximation for the modal metric is very tight over different channel correlations and modulations.

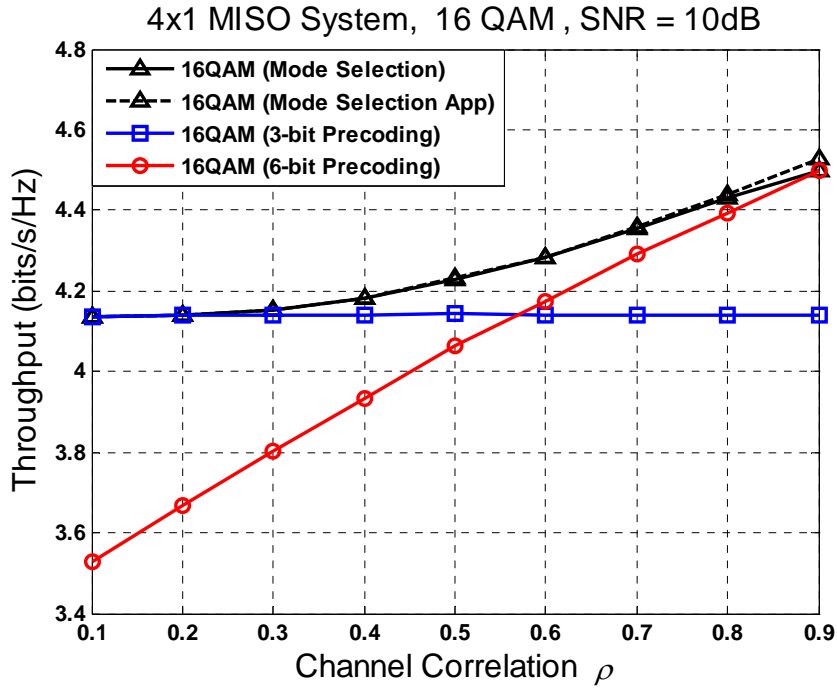


Fig. 4-5 Dual-mode scheme, Dual-mode scheme with approximated modal metric and single-mode scheme with SNR = 10dB and 16 QAM

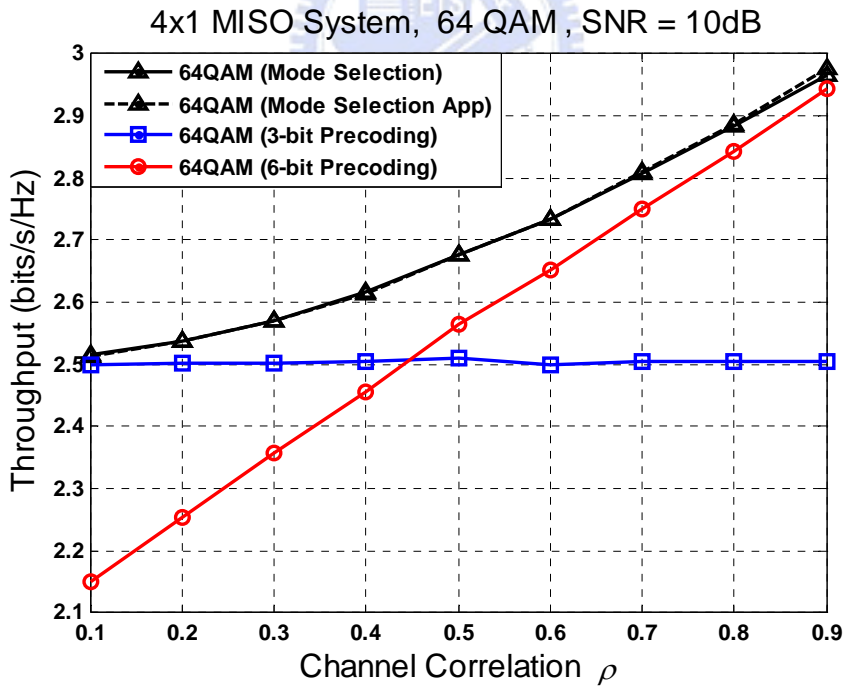


Fig. 4-6 Dual-mode scheme, Dual-mode scheme with approximated modal metric and single-mode scheme with SNR = 10dB and 64 QAM

### 4.3.4 Throughput-Based Criterion vs. Other Criteria

To compare the proposed criterion with other selection criteria, we give the following simulations. First, we consider a randomly-selecting criterion which randomly selects one mode for use per two frames and the simulation result is given in Fig. 4-7. As expected, the system performance with randomly-selecting criterion is between 3-bit precoding scheme and 6-bit precoding scheme since two modes are used with the same probability. Also, the proposed throughput-based criterion outperforms the randomly-selecting criterion.

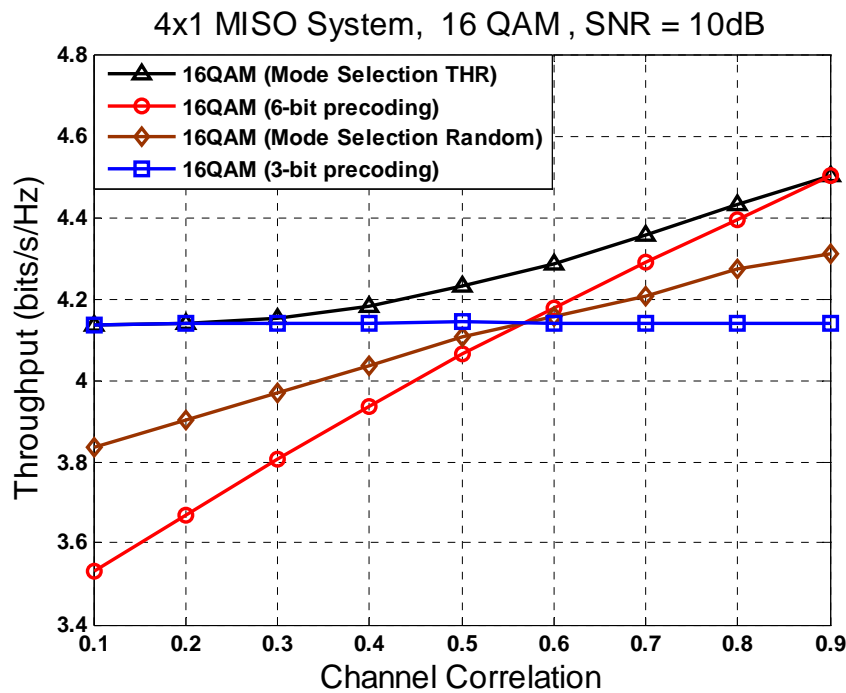


Fig. 4-7 Throughput-based criterion and random selection

Secondly, we consider the SER-based criterion considered in [11], and the simulation results are given in Fig. 4-8 and Fig. 4-9. By using the proposed throughput-based criterion, the system performance is comparable to that using the SER-based criterion. However, the proposed selection criterion is more feasible than the SER-based criterion since there is no complex integral involved.

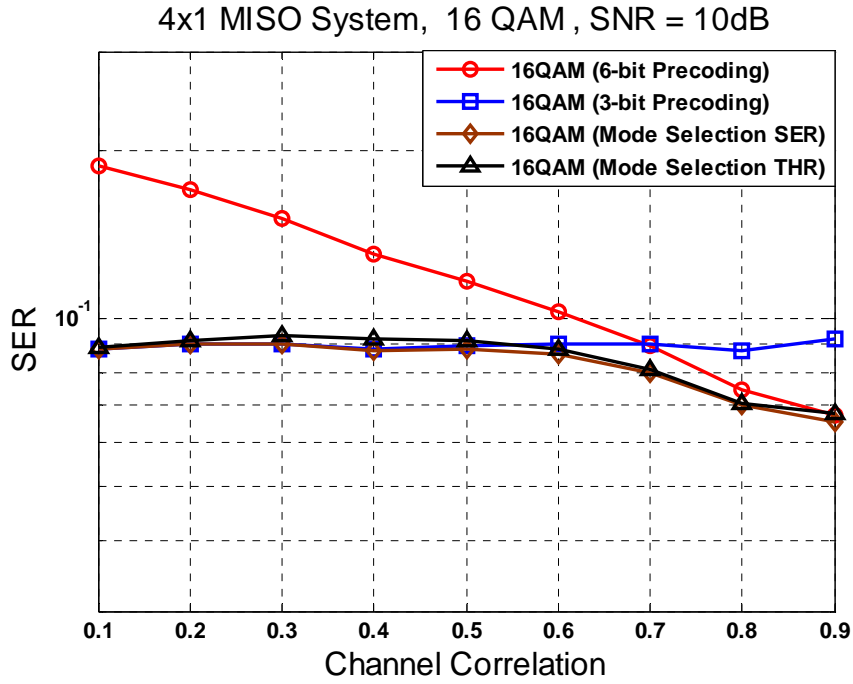


Fig. 4-8 Throughput-based criterion and SER-based criterion in the dual-mode scheme with SNR = 10dB and 16 QAM

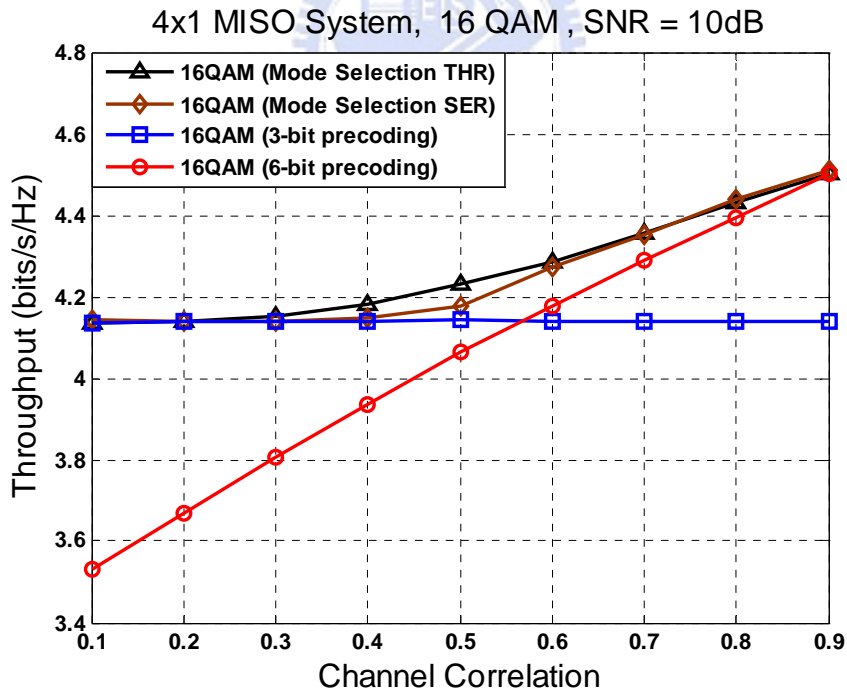


Fig. 4-9 Throughput-based criterion and SER-based criterion in the dual-mode scheme with SNR = 10dB and 16 QAM



## 4.4 Summary

In this chapter, we try to analyze the formulas of the modal metric with respect to Mode I and Mode II given in Chapter 3. Our goal is to find the closed form solutions for them, but unfortunately, to our best knowledge this cannot be obtained. As an alternative, we derive the approximations of the expected value of throughput corresponding to Mode I and Mode II respectively, giving a much practical way to implement the algorithm of selecting the mode at the receiver. The simulation results show that the approximations are very tight throughout all channel correlations, SNRs, and modulations in consideration. Moreover, the proposed criterion performs comparably to other existing mode selection criteria.



# Chapter 5

## Conclusion

Limited feedback communication is a prevailing technique to enhance the system performance through relaying back the CSI over a band-limited channel to the transmitter. In MIMO systems, feedback can be used to assign a pre-designed matrix, i.e., precoder to the transmitter, hence activating the strongest channel mode. One of the approaches to implement this is the codebook-based limited feedback scheme. In this scheme, a pre-designed codebook containing finite numbers of quantized channel matrices is provided at the transmitter and the receiver, so the receiver can pick one precoder from the codebook by some criterions and inform the transmitter of the index of the precoder.

In this thesis, we consider a limited feedback system in which two different sizes of codebooks are used to enhance the system performance. The large codebook contains more precoders, hence a near-optimal precoder can be selected with a higher probability. On the other hand, while the small coderbook contains fewer precoders, it takes fewer bits for the system using Mode II to relay back the corresponding index. Specifically, the inherent problem that the dual-mode scheme would confront in time-varying channel is: feeding back fewer bits more often suffers performance degradation while the channel varies slowly; relaying back more bits less often suffers

performance degradation while the channel varies rapidly. In view of this, we propose a throughput-based mode selection criterion that exploits the information of channel correlations to improve the system performance of the dual-mode scheme.

To simulate a time-varying environment, the first-order Markov channel model is considered in our work. Under this channel model, we assume that the channel condition between two consecutive frames is related to each other with a correlation constant. Under the assumption that the receiver has full CSI at the start of each frame, we propose the modal metric taking account of the channel correlation and use it as a gauge between the two modes. With this modal metric, the receiver is able to choose a suitable mode and decide the frequency of feedback, therefore improve the system performance. Moreover, in order to compute the modal metric in a practical way, two approximations for the modal metric corresponding to Mode I and Mode II are derived in this thesis. The tightness of the approximations is justified by numerical experiments. The main contribution of this work is that an alternative mode selection criterion is proposed to jointly consider two codebooks of different sizes in the limited feedback system. With this criterion, the dual-mode scheme is able to outperform the single-mode scheme over time-varying channels. And mostly important, the dual-mode scheme using the proposed criterion has a comparable performance to those using existing criteria, which are less feasible.

The possible extensions of the proposed work are: (1) Take into account the non-ideal effects of the feedback channels, for examples, time delay and transmission errors, etc.; (2) The MISO system considered in our work can be extended to MIMO systems, and different criteria for mode selection can be proposed to further improve the system performance; (3) The assumption of perfect CSI at the receiver is not realistic. Therefore, the modal metric should be modified to consider the errors of CSI.

# Bibliography

- [1] G. D. Golden, G. J. Foschini, and R. A. Valenzuela, "VBLAST: An architecture for realizing very high data rates over the rich-scattering wireless channel " in *Proc. IEEE ISSSE*, Pisa, Italy, Sep. 1998.
- [2] R. W. Heath and A. Paulraj, "A simple scheme for transmit diversity using partial channel feedback," in *Proc. of IEEE Annual Asilomar Conf. on Signals, Systems, and Computers*, Nov. 1998 .
- [3] A. Narula, M. J. Lopez, M. D. Trott, and G. W. Wornell, "Efficient use of side information in multiple-antenna data transmission over fading channels," *IEEE Jour. Select. Areas in Comm.*, vol. 16, pp. 1423-1436, Oct. 1998.
- [4] A.-Y. Chun Kin and D. J. Love, "On the performance of random vector quantization limited feedback beamforming in a MISO system," *IEEE Trans Wireless Comm.*, vol. 6, pp. 458-462, Feb. 2007.
- [5] K. K. Mukkavilli, A. Sabharwal, E. Erkip, and B. Aazhang, "On beamforming with finite rate feedback in multiple-antenna systems," *IEEE Trans. Inf. Theory*, vol. 49, pp. 2562-2579, Oct. 2003.
- [6] S. A. Jafar and A. Goldsmith, "On optimality of beamforming for multiple antenna systems with imperfect feedback," in *Proc. Int. Symp. Information Theory*, June 2001, pp. 321.
- [7] G. Jongren, M. Skoglund, and B. Ottersten, "Combining beamforming and orthogonal space-time block coding," *IEEE Trans. Inf. Theory*, vol. 48, pp. 611-627, Mar. 2002.
- [8] A. L. Moustakas and S. H. Simon, "Optimizing multiple-input single-output (MISO) communication systems with general Gaussian channels: Nontrivial covariance and nonzero mean," *IEEE Trans. Inf. Theory*, vol. 49, pp. 2770-2780, Oct. 2003.

- [9] D. J. Love and R. W. Heath, "Limited feedback unitary precoding for spatial multiplexing systems," *IEEE Trans. Inf. Theory*, vol. 51, pp. 2967-2976, Aug. 2005.
- [10] IEEE Std 802.16eTM-2005 and IEEE Std 802.16TM-2004/Cor1-2005, "Part 16: Air Interface for Fixed and Mobile Broadband Wireless Access Systems," pp. 587-596, 2005.
- [11] L.-Y. Chen, "Transmit beamforming with dual-mode limited feedback over temporally-correlated channels," Department of Communication Engineering National Chiao Tung University, 2007.
- [12] D. J. Love, R. W. Heath, Jr., and T. Strohmer, "Grassmannian beamforming for multiple-input multiple-output wireless systems," *IEEE Trans. Inf. Theory*, vol. 49, pp. 2735-2747, Oct. 2003.
- [13] W. Santipach and M. L. Honig, "Asymptotic performance of MIMO wireless channels with limited feedback," *Proc. MILCOM*, vol. 1, Boston, MA, Oct. 2003, pp. 141-146.
- [14] V. Raghavan, R. W. Heath, and A. V. Sayeed M, "Systematic codebook designs for quantized beamforming in correlated MIMO channels," *IEEE Jour. Select. Areas in Comm.*, vol. 25, pp. 1298-1310, Sep. 2007.
- [15] K. E. Baddour and N. C. Beaulieu, "Autoregressive modeling for fading channel simulation," *IEEE Trans. Wireless Comm.*, vol. 4, pp. 1650-1662, July 2005.
- [16] G. L. Stuber, *Principles of Mobile Communication*, 2nd ed.: Kluwer Academic Publishers, 2001.
- [17] S. H. Ting, K. Sakaguchi, and K. Araki, "A Markov-Kronecker model for analysis of closed-loop MIMO systems," *IEEE Commun. Lett.*, vol. 10, pp. 617-619, Aug. 2006.
- [18] "IEEE P802.11 Wireless LANs TGn Channel Models."
- [19] J. G. Proakis, *Digital Communications*, 4th ed.: McGraw-Hill, 2001.

- [20] N. L. Johnson, S. Kotz, and A. W. Kemp, *Continuous Univariate distributions*, 2nd ed. vol. 2: Wiley-Interscience, 1994.
- [21] I. S. Gradshteyn and I. M. Ryzhik, *Table of Integrals, Series, and Products*: Academic Press, 2007.
- [22] T. T. Soong, *Fundamentals of Probability and Statistics for Engineers*: Wiley, 2004.
- [23] H. Stark and J. W. Woods, *Probability and Random Processes with Applications to Signal Processing*, 3rd ed.: Prentice Hall, 2002.
- [24] M. Chiani and D. Dardari, "Improved exponential bounds and approximation for the Q-function with application to average error probability computation," *Proc. GLOBECOM'02*, Taipei (Taiwan), Nov. 2002
- [25] S. M. Kay, *Fundamentals of Statistical Signal Processing: Estimation Theory* vol. 1: Prentice Hall, 1993.

